Accepted Manuscript

Design, synthesis, molecular docking and cytotoxic evaluation of novel 2-furybenzimidazoles as VEGFR-2 inhibitors

Mona A. Abdullaziz, Heba T. Abdel-Mohsen, Ahmed M. El Kerdawy, Fatma A.F. Ragab, Mamdouh M. Ali, Sherifa M. Abu-bakr, Adel S. Girgis, Hoda I. El Diwani

PII: S0223-5234(17)30342-2

DOI: 10.1016/j.ejmech.2017.04.068

Reference: EJMECH 9419

To appear in: *European Journal of Medicinal Chemistry*

Received Date: 24 January 2017

Revised Date: 28 March 2017

Accepted Date: 20 April 2017

Please cite this article as: M.A. Abdullaziz, H.T. Abdel-Mohsen, A.M. El Kerdawy, F.A.F. Ragab, M.M. Ali, S.M. Abu-bakr, A.S. Girgis, H.I. El Diwani, Design, synthesis, molecular docking and cytotoxic evaluation of novel 2-furybenzimidazoles as VEGFR-2 inhibitors, *European Journal of Medicinal Chemistry* (2017), doi: 10.1016/j.ejmech.2017.04.068.

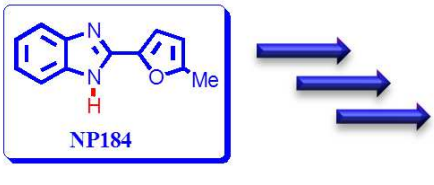

NP184

MCF-7 IC_{50} = 55.55 µM
HepG-2 IC_{50} = 102.53 µM
% inhibition of VEGFR-2 = 39%

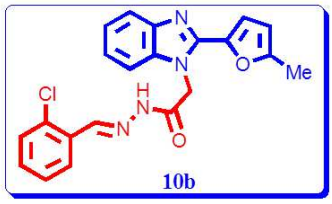

10b

MCF-7 IC_{50} = 21.25 µM
HepG-2 IC_{50} = 22.58 µM
% inhibition of VEGFR-2 = 96%

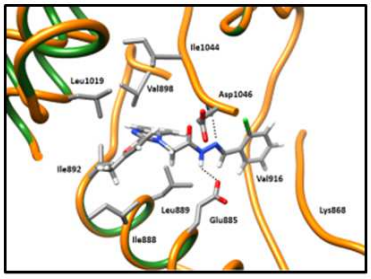

Design, Synthesis, Molecular Docking and Cytotoxic Evaluation of Novel 2-Furybenzimidazoles as VEGFR-2 Inhibitors

Mona A. Abdullaziz,[a] **Heba T. Abdel-Mohsen,***[a] **Ahmed M. El Kerdawy,**[b,c] **Fatma A. F. Ragab,**[b] **Mamdouh M. Ali**,[d] **Sherifa M. Abu-bakr,**[a] **Adel S. Girgis,**[e] **Hoda I. El Diwani**[a]

[a]*Department of Chemistry of Natural and Microbial Products, Division of Pharmaceutical and Drug Industries, National Research Centre, Dokki, Cairo, Egypt*
[b]*Department of Pharmaceutical Chemistry, Faculty of Pharmacy, Cairo University, Kasr El-AiniStreet, Cairo, P.O. Box 11562, Egypt.*
[c]*Molecular Modeling Unit, Faculty of Pharmacy, Cairo University, Kasr El-Aini Street, Cairo, P.O. Box 11562, Egypt.*
[d]*Department of Biochemistry, Division of Genetic Engineering and Biotechnology, National Research Centre, Cairo, Egypt*
[e]*Department of Pesticide Chemistry, Division of Chemical Industries Research, National Research Centre*
**Corresponding author: Email address: hebabdelmohsen@gmail.com*

Abstract

Inhibition of angiogenesis through inhibition of vascular endothelial growth factor receptor 2 (VEGFR-2) has been applied in cancer therapy because of its important role in promoting cancer growth and metastasis. In the presented study, a series of benzimidazol-furan hybrids was designed and synthesized through facile synthetic pathways. Evaluation of the synthesized compounds for their *in vitro* cytotoxic activity against breast (MCF-7) and hepatocellular (HepG2) carcinoma cell lines was performed. Two of the synthesized conjugates, **10b** and **15**, showed potent antiproliferative properties against MCF7 cell line (IC_{50} = 21.25, 21.35 µM, respectively) in comparison to tamoxifen (IC_{50} = 21.57 µM). Additionally, compounds **10a**, **10b**, **15** and **17** showed promising potency (IC_{50} = 25.95, 22.58, 26.94 and 31.06 µM, respectively) against liver carcinoma cell line HepG2 in contrast to cisplatin (IC_{50} = 31.16 µM). Moreover, *in vitro* evaluation of the synthesized compounds for their effect on the level of VEGFR-2 in MCF-7 cell line showed their potent inhibitory activity relative to control untreated cells. Four compounds **10a, 10b, 14** and **15** showed 92-96% reduction in VEGFR-2 level, compared with tamoxifen and sorafenib which showed inhibition percentage of 98% and 95.75%, respectively. Compound **10a** was found to have promising VEGFR-2 inhibitory activity (IC_{50} = 0.64 µM) in comparison to sorafenib (IC_{50} = 0.1 µM). Molecular docking was performed to study the binding pattern of the newly synthesized compounds with VEGFR-2 active site. Molecular docking attributed their good VEGFR-2 inhibitory activity to their hydrogen bonding interaction with the key amino acids in VEGFR-2 active site, Glu885 and Asp1046, and their hydrophobic interaction by their 2-furylbenzimidazole moiety with the allosteric hydrophobic back pocket in a type III

inhibitors-like binding mode. The binding interaction is augmented by a ring substituent with long chain extension at position 1 of the benzimidazole due to its hydrophobic interaction with the hydrophobic side chains of the amino acids at the interface between the ATP binding site and the allosteric back pocket. Structure-activity relationship (SAR) was inferred for future optimization based on the performed biological and docking studies.

Key words: Angiogenesis; VEGFR-2; 2-Furylbenzimidazole; MCF-7; HepG-2

1. Introduction

Cancer is becoming one of the most serious health problems in the world. Moreover, adverse effects of classical non-selective chemotherapies and resistance development for the existing anticancer drugs make the search for more selective new anticancer agents an urgent research point. However, designing a molecule that can selectively inhibit the proliferation of abnormal cells only with little or no effect on normal cells is a difficult task [1].

Angiogenesis, the formation of new blood vessels from pre-existing ones, is a normal physiological process taking place during embryogenesis, inflammation and wound healing. On the other hand, pathological angiogenesis is associated with many disease conditions such as cancer, where new blood vessels infiltrate tumor masses supplying them with oxygen and nutrients to enhance tumor growth and metastasis [2-4]. Hence, blocking angiogenesis could be a strategy to hinder tumor growth. Unlike classical chemotherapy, which causes severe adverse effects and leads to drug resistance with long-term treatment, angiogenesis inhibition could be more effective in preventing tumor progression and well-tolerated [2-5].

Numerous growth factors are involved in angiogenesis. One of the most known angiogenic molecules is the vascular endothelial growth factor (VEGF) family members which are pivotal stimuli of physiological as well as pathological angiogenesis [4]. Vascular endothelial growth factor (VEGF) regulates blood and lymphatic vessel development and homeostasis [5,6]. VEGF ligands bind in an overlapping pattern to three different, but structurally related, VEGF-receptor tyrosine kinases (VEGFR-TK) which are VEGFR-1 (FLT1), VEGFR-2 (KDR/FLK1) and VEGFR-3 (FLT4) [7].

VEGFR-2, a type III transmembrane receptor tyrosine kinase, is vital for angiogenesis [8]. Several complex mechanisms are involved in the regulation of VEGFR-2 levels [9]. Hence, blocking of VEGFR-2 or down regulation of its signaling became a main approach for the discovery of new drugs for many human angiogenesis-dependent malignancies. To date, a humanized anti-VEGF monoclonal antibody (bevacizumab) and several small molecule VEGFR-2 kinase inhibitors (sorafenib, regorafenib, sunitinib, vandetanib, pazopanib, axitinib and cabozantinib) have been approved as anti-angiogenic drugs [10-13]. However, some adverse effects have been observed during their clinical use, such as bleeding complications, indicating that development of safer VEGFR-2 inhibitors is still an active field of research.

As a member of the protein tyrosine kinase family, VEGFR-2 intracellular domain (catalytic domain) has the conservative bi-lobed structure observed in all protein kinases (C-terminal lobe and N-terminal lobe). The catalytic cleft is formed between these two lobes and consists of residues contributed by both lobes [14]. The kinase domain has an ATP binding cleft located between these two lobes. The C-terminal lobe contains an activation loop (A-loop) marked by a conserved triad aspartate-phenylalanine-glycine (DFG) motif located at its beginning [15]. The A-loop can adopt numerous conformations and according to the 3D orientation of the DFG motif, the protein kinase structure can be found in the active or inactive conformation [16,17]. In the active state (DFG-in), the A-loop is positioned away from the catalytic center (open conformation) exposing the residues responsible for the protein substrate binding, simultaneously, it directs the catalytic aspartic acid into the ATP binding pocket. Upon DFG motif flipping into an inactive (DFG-out) conformation, the A-loop adapts a closed conformation leaving behind a hydrophobic back pocket nearby the ATP-binding cleft [16]. This hydrophobic pocket is important for the binding of a group of the tyrosine kinase inhibitors [16].

Generally, VEGFR-2 inhibitors are classified according to whether they competitively bind to the ATP binding pocket in the active “DFG-in” conformation (type I) or the inactive “DFG-out” conformation (type II), or noncompetitively via binding outside the ATP binding pocket in the allosteric hydrophobic back pocket (type III) [15-18]. Type I inhibitors act on the active “DFG-in” conformation via hydrogen bonding with the hinge region amino acid Cys919 and hydrophobic interactions in and around the adenine region [17]. Type II inhibitors such as sorafenib occupy the ATP binding site and extend over the gatekeeper Val916 into the adjacent allosteric hydrophobic

back pocket in the inactive "DFG-out"conformation [17-20]**.** Type III inhibitors bind to the inactive "DFG-out"conformation beyond the gatekeeper Val916 exclusively to the less conservative allosteric hydrophobic back pocket outside the ATP binding pocket locking VEGFR-2 in the inactive "DFG-out"conformation. Therefore, they are expected to have superior selectivity profiles and offer new opportunities for scaffold development [17,20].

Over the last few years, a wide range of VEGFR-2 inhibitors have been designed and synthesized [21-23]. For example, 2-furylbenzimidazoles were reported as promising anti-angiogenic agents through VEGFR-2 inhibition. 2-(5-Methylfuran-2-yl)-1*H*-benzimidazole (NP-184) was reported as a potent anti-angiogenic agent. It was discovered to reduce the angiogenesis *in vivo* in material plug assay model [24,25]. PJ-6 was also found to inhibit endothelial cells proliferation and migration when evaluated for its anti-angiogenic activity. Also, PJ-8, 5-benzoyl-2-(5-methyl-2-furyl)-1*H*-benzimidazole significantly inhibited VEGFR-2 and suppressed tumor-induced angiogenesis *in vivo* (Figure 1) [26].

The present work is a continuation of our effort to design novel anti-angiogenic 2-furylbenzimidazoles [27,28]. This pursue is inspired by our development of the effective 2-furylbenzimidazole derivatives **A** and **B** (Figure 1) which have structural resemblance to NP-184 [24,25], Pj-6 and Pj-8 [26]. Compounds **A** and **B** showed more potent antitumor properties against breast carcinoma cell line MCF-7 than tamoxifen as well as potent anti-angiogenic activity against VEGFR-2 [27,28].

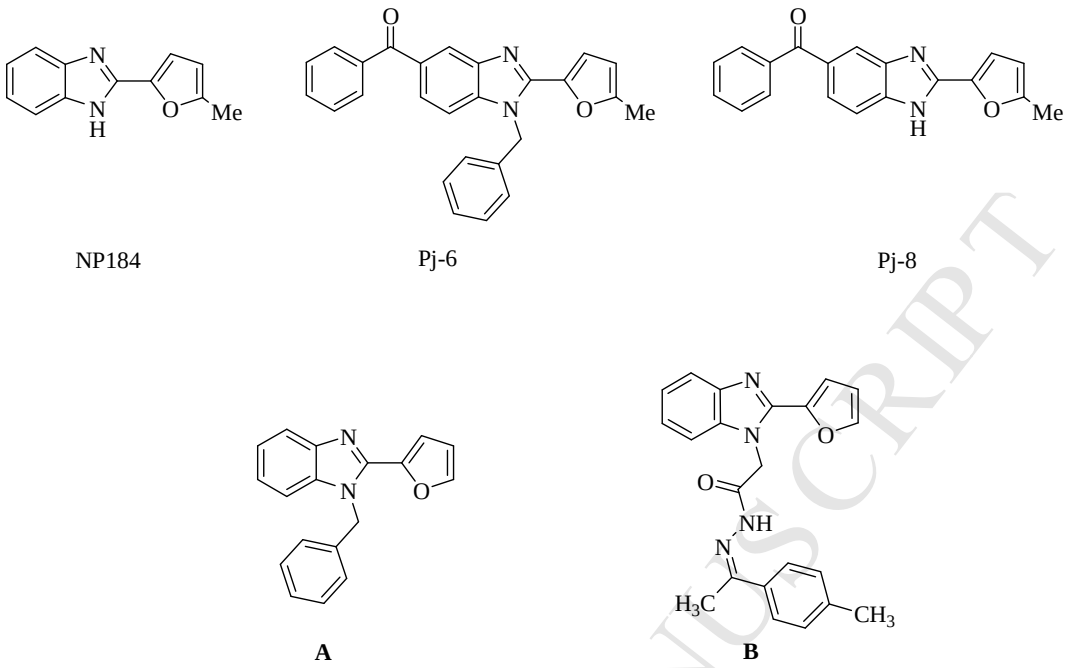

Figure 1. Anti-angiogenicbenzimidazole based-compounds

The VEGFR-2 inhibitory activity of this series is assumed to be mediated through accommodation of the benzimidazole ring into the allosteric hydrophobic back pocket of the VEGFR-2 in the inactive "DFG-out" conformation [27] as was inferred from X-ray crystallography and molecular docking studies [27,29]. Increasing the hydrophobicity of the benzimidazole ring for instance by addition of trifluoromethyl substitution leads to increase in the VEGFR-2 inhibitory activity as it increases the hydrophobic interaction with the hydrophobic pocket [29]. Further interactions may also take place with the side chain carboxylate of Glu885 of the αC helix and/or with Asp1046 in the conserved DFG motif through hydrogen bonding with the appropriate moieties in the inhibitors [27,29].

In the current work, starting from the reported inhibitor NP184 in figure 1, new analogues were designed (Figure 2), such that modification on the benzimidazole ring was carried out through the introduction of various hydrophobic groups such as alkyl, phenyl and heterocyclic ring systems through a spacer or without a spacer in position 1. Also, substitution at position 5 of the furyl moiety was carried out with a methylene morpholino group. The aim of this suggested modification was to increase the hydrophobic nature of the newly synthesized derivatives in order to increase their binding affinity to VEGFR-2 through increasing the hydrophobic interaction with its allosteric hydrophobic back pocket.

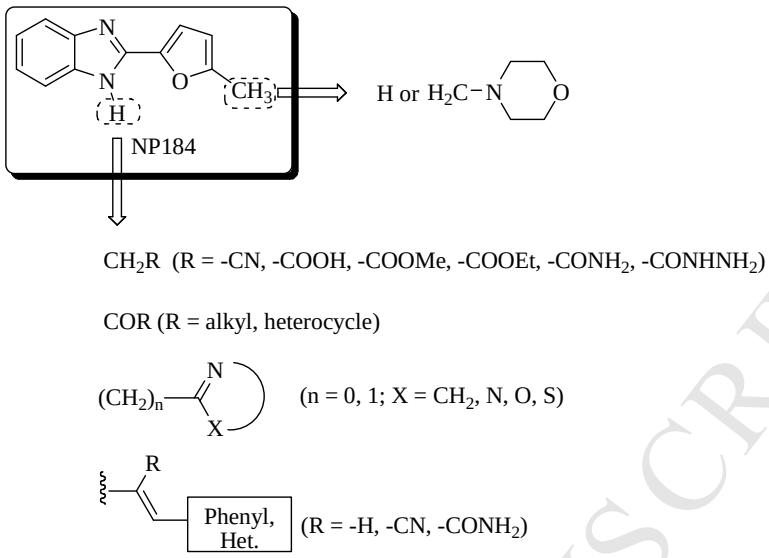

Figure 2. Schematic representation showing the designing strategy of 2-(2-furyl)-1*H*-benzimidazoles

The designed novel 2-furylbenzimidazole derivatives were synthesized and their antitumor activity against MCF7 (breast) and HepG2 (hepatocellular) carcinoma cell lines was evaluated. Moreover, *in vitro* evaluation of the synthesized compounds for their effect on the level of VEGFR-2 in MCF-7 cell line was carried out.

Molecular docking studies were performed to find out the possible binding mode of the newly synthesized compounds with VEGFR-2, and to study their interaction with the receptor hot spots (key amino acids) with the aim of explaining their VEGFR-2 inhibitory activity.

2. Results and Discussion

2.1. Chemistry

2-Furylbenzimidazoles **4a**,**b** were synthesized by the reaction of furfural bisulfite adducts **2a**,**b** with 1,2-phenylenediamine (**3**) under reflux [28,30,31]. Treatment of the benzimidazoles **4a**,**b** with either ethyl or methyl bromoacetate afforded the *N*-alkylated products **5a**,**b** or **6a**,**b**, respectively [27]. Hydrolysis of the formed methyl esters **6a**,**b** to the corresponding carboxylic acids **7a**,**b** was achieved by refluxing in methanol under basic conditions. Reaction of the esters **5a**,**b** with hydrazine hydrate afforded the 1*H*-benzo[*d*]imidazol-1-yl-acetohydrazides **8a,b**. Cyclization of the acid hydrazides **8a**,**b** to the corresponding oxadiazoles **9a**,**b** was achieved by their reaction with formic acid or trichloroacetic acid in the presence of $POCl_3$, respectively. The acid hydrazides **8a**,**b** were also

condensed with 2-chlorobenzaldehyde under basic conditions to afford the Schiff bases **10a**,**b**, respectively (Scheme 1).

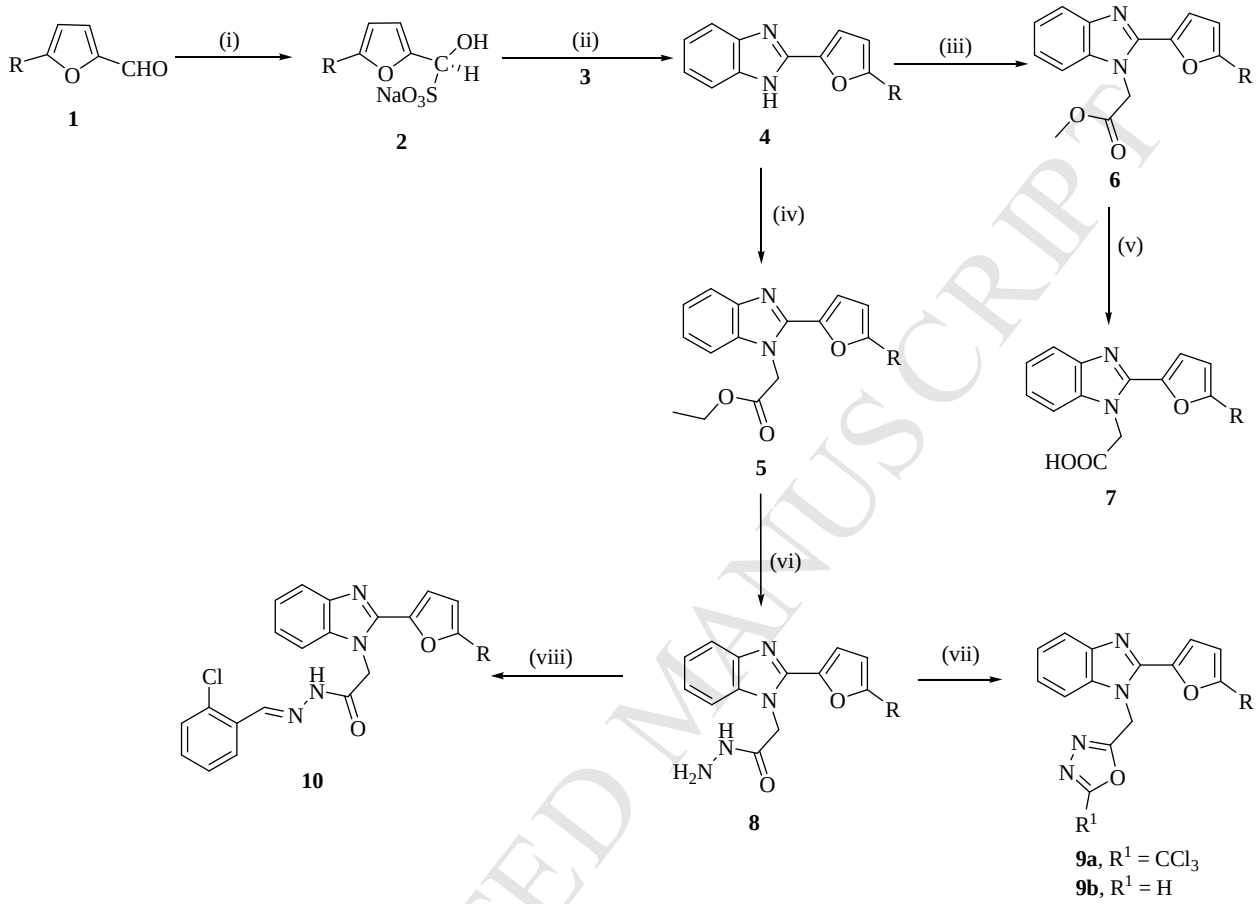

Reagents and conditions: (i) $Na_2S_2O_5$, H_2O, methanol, stirring, r.t., 15 min; (ii) 1,2-phenylenediamine, DMF, reflux, 4 h; (iii) $BrCH_2COOMe$, anhydrous K_2CO_3, acetone, reflux, 8 h; (iv) $BrCH_2COOEt$, anhydrous K_2CO_3, acetone, reflux, 8 h; (v) methanol, anhydrous K_2CO_3, reflux, 4 h; (vi) $NH_2NH_2.H_2O$, methanol, reflux, 4 h; (vii) R^2COOH, $POCl_3$, reflux, 20 h; (viii) 2-Chlorobenzaldehyde, 10% NaOH, ethanol, stirring, r.t., 4 h.

Scheme 1. Synthesis of benzimidazole-furan hybrids **4-10**

Cyanomethylation of **4a** by chloroacetonitrile in the presence of anhydrous potassium carbonate in dry acetone gave the benzimidazole derivative **11.** Subsequently, **11** was reacted with hydrazine hydrate to give the acetimidohydrazide derivative **12**. The thiadiazole derivative **13** was obtained by a cyclization reaction of **12** with carbon disulphide in the presence of potassium hydroxide. Alkylation of **13** with ethyl bromoacetate, in acetone containing anhydrous potassium carbonate, gave ethyl-2-((5-((2-(furan-2-yl)-1*H*-benzo[*d*]imidazol-1-yl)methyl)-1,3,4-thiadiazol-2-ylthio)acetate (**14)** which

was converted to the corresponding hydrazide **15** by refluxing with hydrazine hydrate in methanol (Scheme 2).

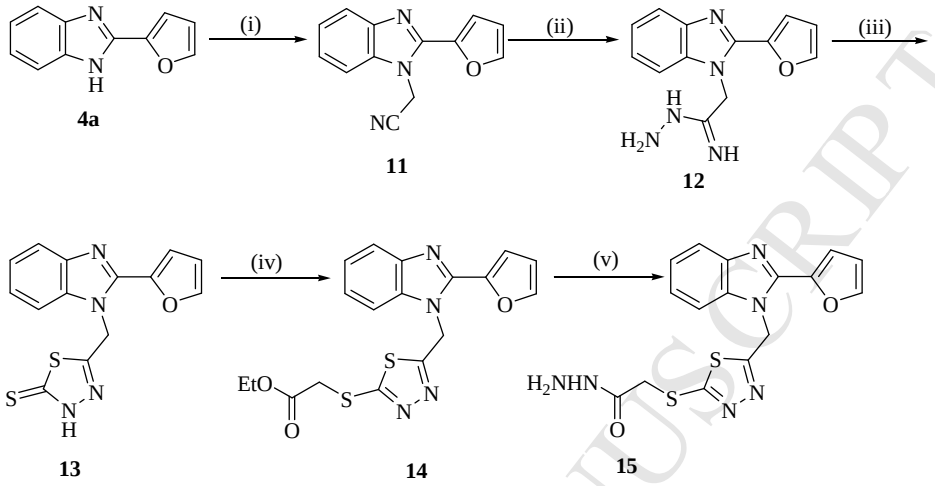

Reagents and conditions: (i) $ClCH_2CN$, anhydrous K_2CO_3, acetone, reflux, 8 h; (ii) $NH_2NH_2.H_2O$, methanol, reflux, 4 h; (iii) CS_2, KOH, ethanol, reflux, 10 h; (iv) $BrCH_2COOEt$, anhydrous K_2CO_3, acetone, reflux, 4 h; (v) $NH_2NH_2.H_2O$, methanol, reflux, 4 h.

Scheme 2. Synthesis of benzimidazole-furan hybrids **11-15**

2-(2-(Furan-2-yl)-1*H*-benzo[*d*]imidazol-1-yl)-2-(4-oxo-3-phenylthiazolidin-2-ylidene)acetonitrile **(16)** was obtained through reaction of the cyanomethyl derivative **11** with phenylisothiocyanate followed by cyclization using ethyl bromoacetate. Formation of the thiazolidine-4 one derivative **17** was performed by the reaction of **11** with thioglycolic acid. Hydrolysis of **11** to the corresponding amide was achieved by refluxing with piperidine in ethanol. Knoevenagel condensation of **18** with benzaldehyde or 2-chlorobenzaldehyde under basic condition yielded the corresponding ylidenes **19a**,**b**, respectively (Scheme 3).

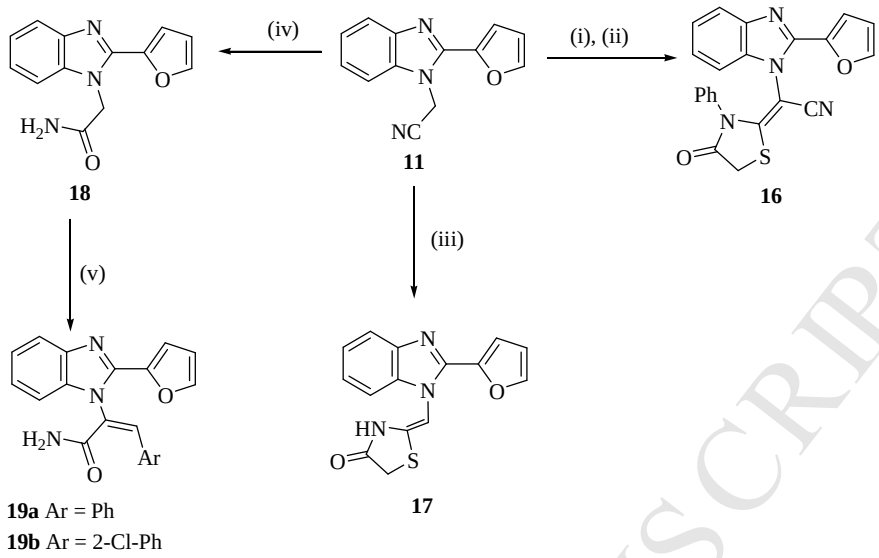

Reagents and conditions: (i) Phenyl isothiocyanate, KOH, DMF, r.t., 30 min; (ii) $BrCH_2COOEt$, stirring, 2 h; (iii) $SHCH_2COOH$, glacial acetic acid, ethanol, reflux, 8 h; (iv) Ethanol, piperidine, reflux, 8 h; (v) RCHO, 10 % KOH solution, ethanol, stirring, r.t., 4 h.

Scheme 3. Synthesis of benzimidazole-furan hybrids **16-19**

Aminoalkylation of the furan ring of **4a** using morpholine and paraformaldehyde was achieved giving **20**. 2-Chloro-1-(2-(furan-2-yl)-1*H*-benzo[*d*]imidazol-1-yl)ethan-1-one (**21**) was synthesized by substitution reaction of the imidazolyl NH of **4a** with chloroacetyl chloride. Compound **21** was reacted with thiosemicarbazide or guanidine hydrochloride to afford the corresponding cyclized products **22** and **23**, respectively (Scheme 4).

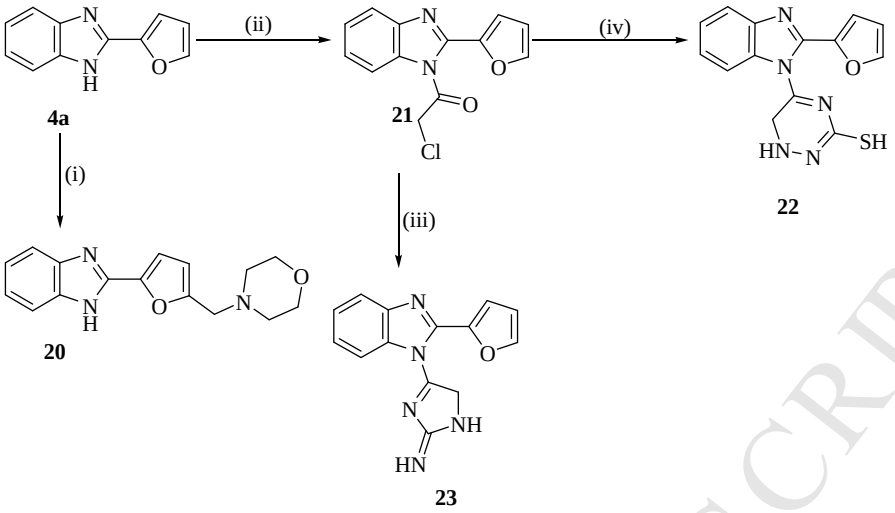

Reagents and conditions: (i) Morpholine, paraformaldehyde, HCl, methanol, reflux, 2 h; (ii) Chloroacetyl chloride, anhydrous K_2CO_3, acetone, stirring, r.t., 8 h; (ii) Thiosemicarbazide, anhydrous K_2CO_3, acetone, stirring, r.t., 8 h; (iv) Guanidine.HCl, K_2CO_3 anhydrous, acetone, stirring, r.t., 8 h.

Scheme 4. Synthesis of benzimidazole-furan hybrids **20-23**

Dimerization of 5-methyl-2-furyl-benzimidazole (**4b**) was achieved by its reaction with 0.5 equivalent diethyl carbonate or diethyl oxalate under acidic conditions to give the bis-benzimidazoles**24** and **25**, respectively (Scheme 5).

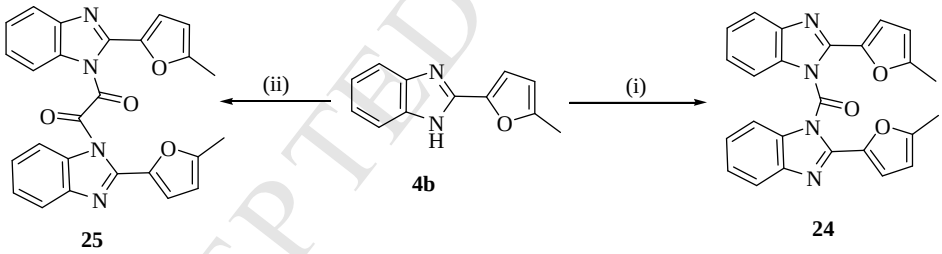

Reagents and conditions: (i) Diethyl carbonate, ethanol, conc. HCl, stirring, r.t., 5 h;
(ii) Diethyl oxalate, ethanol, conc. HCl, stirring, r.t., 5 h.

Scheme 5. Synthesis of bisbenzimidazoles **24, 25**

2.2. Biological Studies

2.2.1. *In vitro* anti-proliferative activity

The synthesized benzimidazoles were evaluated for their *in vitro* cytotoxic activity against human breast cancer cell line MCF-7 and liver carcinoma cell line HepG-2 using SRB assay [32,33]. The IC_{50} values of the tested compounds as well as the positive controls are summarized in Table 1.

From the data obtained (Table 1), it is obvious that compounds **10b** and **15** exhibited promising activities (IC_{50} = 21.25 and 21.35µM, respectively) against breast carcinoma cell line MCF7 with in comparison to tamoxifen (IC_{50} = 21.57µM). Additionally, compounds **10a**, **14** and **17** (IC_{50} = 26.05, 28.50 and 29.13 µM, respectively) showed mild activities against MCF-7. Compounds **10a**, **10b**, **15** and **17** showed higher potency (IC_{50} = 25.95, 22.58, 26.94 and 31.06 µM, respectively) than that of cisplatin (IC_{50} = 31.16 µM) against liver carcinoma cell line HepG2.

2.2.2. *In vitro* effect of the synthesized compounds on the level of VEGFR-2 in MCF-7 cell line

Vascular endothelial growth factor (VEGF) and vascular endothelial growth factor receptor (VEGFR-2) stimulate angiogenesis in tumor tissues thus promoting their nourishment and progression [34,35]. Recent studies demonstrated that VEGFR-2 is up-regulated in MCF-7 cell line [36]. The effect of the newly synthesized molecules as well as tamoxifen, which was previously reported to have anti-angiogenic effect through inhibition of VEGFR-2 [37,38], on the level of human vascular endothelial growth factor receptor (VEGFR-2) was determined utilizing breast cancer cell line MCF-7 obtained from the American Type Culture Collection (Rockville, MD, USA)**.** This biological study was undertaken utilizing double-antibody sandwich enzyme-linked immunosorbent assay (ELISA) to assay the level of human VEGFR-2 in treated human breast cancer cell line MCF-7 samples as compared to the level in the untreated cells. The observed results were depicted in Table 1. Most of the tested compounds showed considerable inhibitory activity. Four compounds **10a**,**b, 14**, and **15** showed 92-96% reduction in VEGFR-2 level in contrast to tamoxifen and sorafenib which showed inhibition percentage of 98% and 95.75%, respectively.

Table 1. *In vitro* cytotoxic activity of the synthesized benzimidazoles against human hepatocellular HepG2 and breast cancer MCF7cell lines as well as their effect on VEGFR-2 level in MCF-7 cell line.

Compd.	HepG-2, IC_{50}[a] (µg/ml, µM)	MCF-7, IC_{50},[a](µg/ml, µM)	VEGFR-2 level (ng/ml)	VEGFR-2 inhibition[c](%)
4a	18.913, 102.53	19.458,105.64	2761.61	43
4b	20.300, 102.54	14.000, 55.55	2980.74	39
5a	>50,>185.19	15.200, 57.29	2210.12	57
5b	>50,>176.06	17.800, 63.53	3520.40	25

6a	21.087, 67.29	20.653, 80.60	1926.33	61
6b	>50, >185.19	23.510, 87.04	3010.51	38
7a	35.963, 148.54	18.913, 63.08	4200.63	61
7b	>50, >195.31	35.610, 139.06	3896.30	20
8a	>50, >195.31	20.200, 79.22	3942.11	19
8b	>50, >185.19	22.400, 68.27	3530.55	24
9a	37.000, 132.14	>50,>177.31	---	---
9b	32.610, 85.57	>50,>130.89	---	---
10a	9.680, 25.95	9.860, 26.05	290.20	94
10b	8.93, 22.58	8.330, 21.25	190.80	96
11	19.524, 88.13	19.524, 88.13	2987.11	39
12	19.022, 74.52	17.391, 53.13	3540.22	27
13	15.000, 47.56	21.304, 52.61	4195.46	14
14	24.458, 62.07	11.413, 28.50	362.80	92
15	10.400, 26.94	8.293, 21.35	210.60	96
16	15.611, 39.60	21.848, 55.87	1480.33	55
17	9.230, 31.06	9.390, 29.13	535.90	86
18	37.568, 157.34	28.355, 117.61	1926.33	13
19a	20.611, 63.04	12.568, 38.62	961.85	80
19b	16.304, 44.82	14.575, 40.04	1358.42	57
20	36.200, 127.9	15.435, 55.46	1329.61	58
21	19.633, 60.89	19.633, 60.89	2910.19	40
22	18.153, 62.05	22.510, 60.52	2910.61	40
23	16.630, 63.54	24.524, 93.02	3790.38	22
24	>50, >118.48	24.200, 58.34	4420.65	9
25	>50, >111.11	29.510, 65.56	4002.00	17
tamoxifen	----	8.000, 21.57	121.51	98
Sorafenib	----	4.33±0.60	206.33±22.10	95.75
cisplatin	9.348, 31.16	---	---	---
DMSO	---	---	4855.00	0

[a]The concentration required to produce 50% inhibition of cell growth compared to control experiments; [b]Data were expressed as mean of four independent experiments; [c] Percentage changes as compared with control untreated cells.

2.2.3. *In vitro* effect of the synthesized compounds on VEGFR-2

2-Furylbenzimidazoles **10a**, **10b**, **15,** which showed high % of inhibition on the level of VEGFR-2 in MCF-7 cell line, were further measured for their ability to inhibit human VEGFR-2 *in vitro* using Enzyme-Linked Immunosorbent Assay. IC_{50} of the tested compounds were depicted in table 2. The results of the tested compounds were compared with sorafenib as a positive control. From the observed results, it was found that **10a** showed promising IC_{50} against VEGFR-2 (IC_{50} = 0.64 µM) in comparison to sorafenib (IC_{50} = 0.1 µM). Compounds **10b** and **15** showed moderate activity, IC_{50} = 1.26 and 1.41 µM, respectively.

Table 2. IC_{50} (µM) of selected compounds on VEGFR-2

Compound	**IC_{50} (µM)[a] against VEGFR-2**
10a	0.64
10b	1.26
15	1.41
Sorafenib	0.1

[a]The concentration required to produce 50% inhibition of cell growth compared to control experiments.

2.3. Molecular docking study and structure activity relationship (SAR)

Molecular docking was carried out with the aim of explaining the promising VEGFR-2 inhibitory activity of the newly synthesized compounds through investigating their binding mode and their interaction with the key amino acids (hot spots) in the active site of the VEGFR-2.

Several crystal structures are available in the protein data bank for VEGFR-2 [16], for this work we selected (PDB ID: 4ASD) [39] which has VEGFR-2 in the inactive "DFG-out" conformation co-crystallized with sorafenib as type II inhibitor. First, validation of the molecular docking protocol was performed by re-docking of the co-crystallized ligand (sorafenib) in the VEGFR-2 active site. The re-docking validation step reproduced the experimental binding pattern of the co-crystallized ligand efficiently indicating the suitability of the used protocol for the planned docking study as demonstrated by the small RMSD of 0.47Å between the docked pose and the co-crystallized ligand (energy score (S) = −15.19 kcal/mol) and by the capability of the docking pose to reproduce all the

key interactions accomplished by the co-crystallized ligand with the key amino acids (hot spots) in the active site (Glu885, Cys919 and Asp1046) (Figure 3)

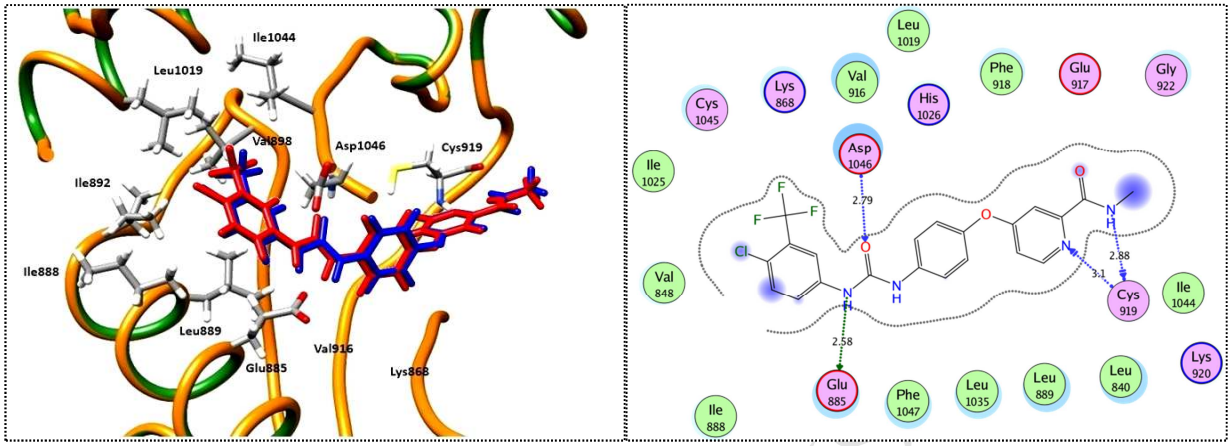

(A) (B)

Figure 3. (A) Superimposition of the docking pose (red) and the co-crystallized (blue)of sorafenib in the VEGFR-2 active site with RMSD of 0.47Å. (B) 2D interaction diagram showing sorafenib docking pose interactions with the key amino acids (hot spots) in the VEGFR-2 active site.(Distances in Å)

Table 3. Docking energy scores (*S*) in kcal/mol for the newly synthesized compounds and the reference compounds in VEGFR-2 active site.

Compound	Energy score (*S*) kcal/mol
4a	-9.02
4b	-9.17
5a	-10.19
5b	-9.96
6a	-9.42
6b	-9.90
7a	-9.67
7b	-10.37
8a	-9.17
8b	-9.43
9a	-10.30

9b	-11.84
10a	-12.34
10b	-13.44
11	-10.63
12	-9.83
13	-10.39
14	-12.38
15	-12.54
16	-13.79
17	-10.94
18	-9.15
19a	-12.29
19b	-13.25
20	-11.22
21	-9.80
22	-11.28
23	-10.35
24	-13.60
25	-14.07
Tamoxifen	-12.05
Sorafenib	−15.19

For compounds **4a**, **4b**, **11** and **20**, the molecular docking study showed a predicted binding pattern involving the fitting of the 2-furylbenzimidazole moiety in the middle of the active site at the interface between the ATP binding site and the allosteric hydrophobic back pocket. Interaction takes place through hydrogen bonding with the side chain carboxylate of Glu885 of the αC helix and with

Asp1046 in the conserved DFG motif (Figure 4). As an exception, compound **11** interacts only with Asp1046 as it has substituted nitrogen at position 1 and not NH as the rest of these compounds.

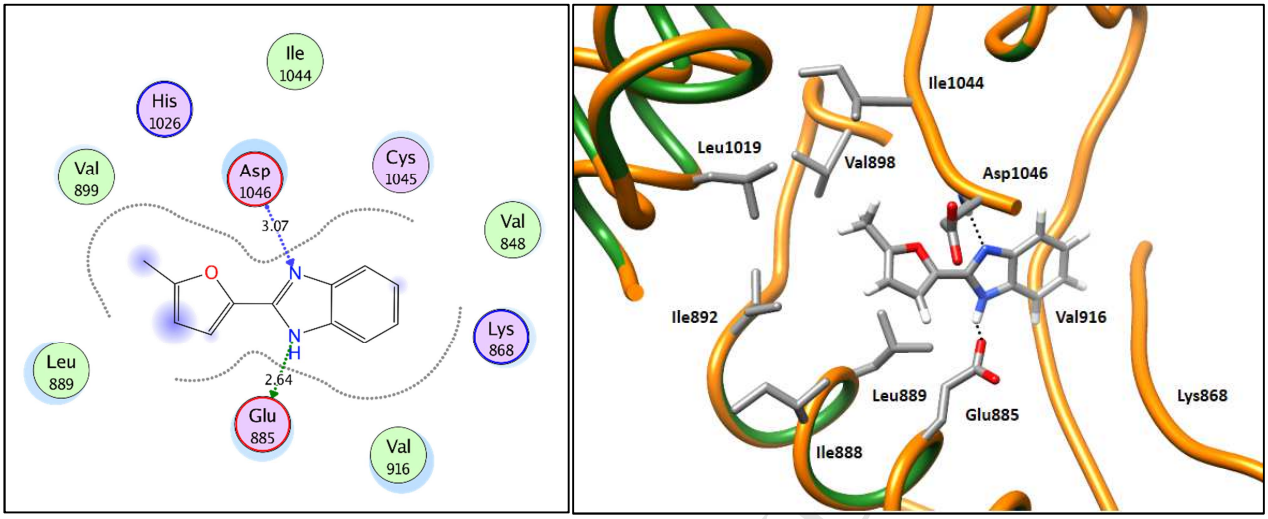

(A) (B)

Figure 4. 2D diagram (A) and 3D representation (B) of compound **4b** showing its interaction with the VEGFR-2 receptor active site (Distances in Å).

Apart from compounds **4a**, **4b**, **11** and **20**, the general predicted binding pattern of the newly synthesized compounds according to the performed docking study involves the accommodation of the 2-furylbenzimidazole moiety in the allosteric hydrophobic back pocket in line with the reported binding mode (Figures 5-7) [27,28]. This binding pattern accomplishes a hydrophobic interaction between the hydrophobic 2-furylbenzimidazole moiety and the hydrophobic back pocket which is lined with the hydrophobic side chains of Ile888, Leu889, Ile892, Val898, Val899, Leu1019 and Ile1044 amino acids achieving the promising VEGFR-2 inhibitory activity of the newly synthesized compounds.

In addition to the 2-furylbenzimidazole hydrophobic interaction, most of the compounds performed further interactions with the VEGFR-2 binding site through hydrogen bonding with the side chain carboxylate of Glu885 of the αC helix and/or with Asp1046 in the conserved DFG motif (Figures 5-7). This type of binding resembles VEGFR-2 type III inhibitors binding mode. (For further details see supporting information).

Compounds **10a** and **10b** showed both the 2-furylbenzimidazole hydrophobic interaction and the hydrogen bonding interactions with the side chain carboxylate of Glu885 and with DFT motif Asp1046 in the active site (figures 5 and 6). Moreover, this binding pattern allows **10a** and **10b** to accommodate their *o*-chlorophenyl moiety in the vicinity of the hydrophobic side chains of Val848, Lys868, Leu889, Val916 and Phe1047 amino acids to be involved in a hydrophobic interaction with these hydrophobic side chains maximizing the binding interaction of both compounds with the VEGFR-2 active site. This binding pattern of compounds **10a** and **10b** ensures that they have the best VEGFR-2 inhibitory activity among the newly synthesized compounds (Table 3).

In compound **10b,** the presence of a 5-methyl substitution on the furan ring increases the hydrophobic interaction with the allosteric hydrophobic back pocket and so increases the binding interaction as can be noticed in its docking score (−13.44 kcal/mol) as compared to that of its analogue **10a** (−12.34 kcal/mol) (Table 3). This superiority is reflected in the effect on VEGFR-2 level as shown in table 1 (VEGFR-2 inhibition % of 98% in **10b** vs. 96% in **10a**).

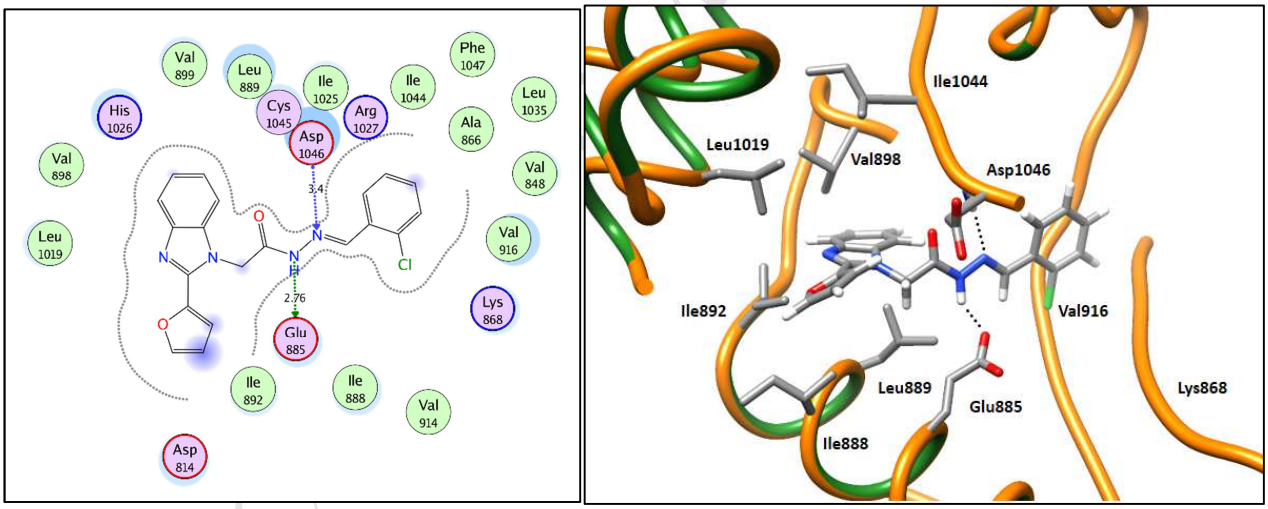

(A) (B)

Figure 5. 2D diagram (A) and 3D representation (B) of compound **10a** showing its interaction with the VEGFR-2 receptor active site. (Distances in Å)

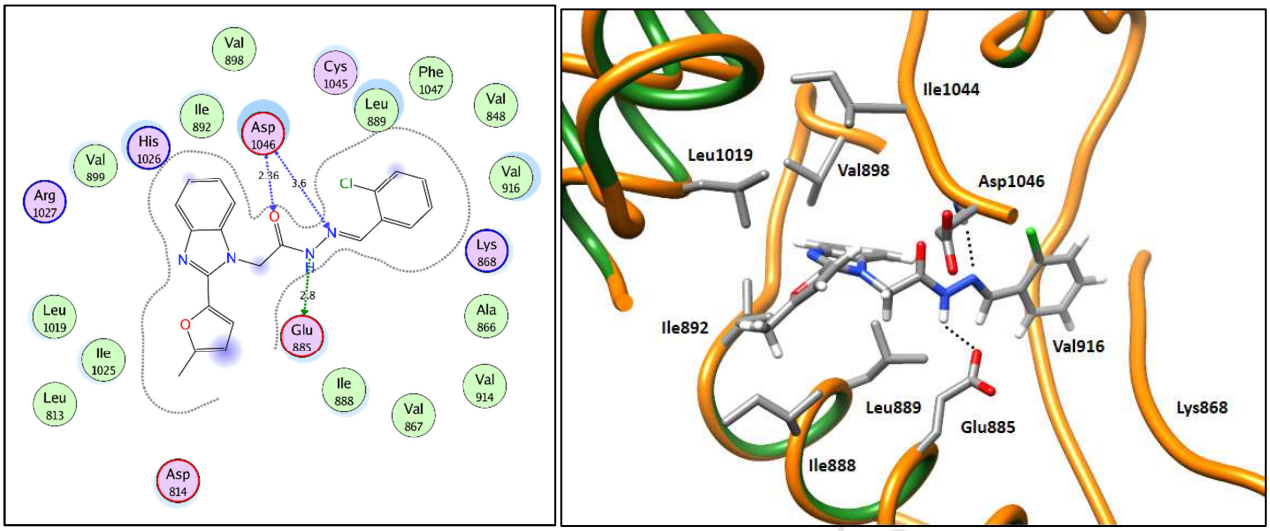

(A) (B)

Figure 6. 2D diagram (A) and 3D representation (B) of compound **10b** showing its interaction with the VEGFR-2 receptor active site. (Distances in Å)

Increasing the size and the hydrophobic nature of the substituent at position 1 of the benzimidazole ring increases the binding interaction with VEGFR-2 active site as indicated by the better docking score of the compounds with cyclic ring substituent as compared to those without ring substituent (e.g. compound **17** vs. **18** with docking score −10.94 vs.−9.15 kcal/mol, respectively and VEGFR-2 inhibition% of 86% vs. 13%, respectively. Also, the binding gets stronger when the ring substituent is extended with a long chain, for example, compounds **14** and **15** with ring substitution (thiadiazole moiety) at position 1 of the benzimidazole ring, extended with ethyl propionate moiety in compound **14** or with acid hydrazide moiety in compound **15,** showed better binding interaction with the active site as indicated in their docking scores (Table 3) compared to that of compound **13** which has no chain extension (−12.38 and−12.54, respectively vs. −10.39 kcal/mol). This higher binding affinity is reflected in their VEGFR-2 inhibitory activity (VEGFR-2 inhibition% = 92% and 96% vs.14% (table 1). Figure 7 shows the binding pattern of compound **15**.

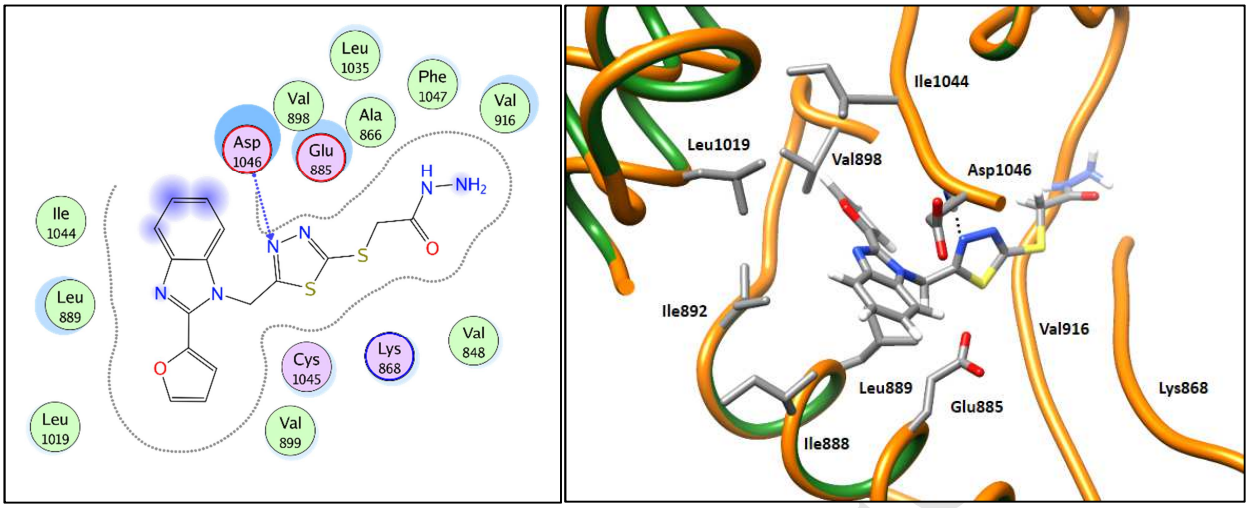

(A) (B)

Figure 7. 2D diagram (A) and 3D representation (B) of compound **15** showing its interaction with the VEGFR-2 receptor active site. (Distances in Å)

In summary, for the 2-furyl-bezimidazoles to achieve high binding affinity (a) 5-Methyl substituent on the furan ring is advantageous to increase the hydrophobic interaction with the allosteric hydrophobic back pocket of VEGFR-2 active site. (b) Suitable hydrogen bond donor and acceptor to interact with Glu885 and Asp1046, respectively. (c) Ring substituent with long chain extension at position 1 of the benzimidazole for hydrophobic binding interaction with the hydrophobic side chains of Val848, Lys868, Leu889, Val916 and Phe1047 amino acids at the interface between the ATP binding site and the allosteric back pocket.

3. Conclusion

2-Furylbenzimidazoles are promising VEGFR-2 inhibitors, from the synthesized series, compounds **10a, 10b, 14** and **15** showed potent reductions in VEGFR-2 level in MCF-7 cell line in comparison to tamoxifen and sorafenib. Compound **10a** was found to have promising VEGFR-2 inhibitory activity (IC_{50} = 0.64 µM) in comparison to sorafenib (IC_{50} = 0.1 µM). Molecular docking attributed their high potency to their type III inhibitors-like binding mode. They bind to the VEGFR-2 active site through hydrogen bonding interaction with the key amino acids in VEGFR-2 active site, Glu885 andAsp1046, and their hydrophobic interaction by their 2-furyl-benzimidazole moiety with the allosteric hydrophobic back pocket which is lined with the hydrophobic side chains of Ile888, Leu889, Ile892, Val898, Val899, Leu1019 and Ile1044 amino acids. The binding interaction is

augmented by the presence of a ring substituent with long chain extension at position 1 of the benzimidazole due to its hydrophobic interaction with the hydrophobic side chains of Val848, Lys868, Leu889, Val916 and Phe1047 amino acids at the interface between the ATP binding site and the allosteric back pocket.

4. Experimental

All chemicals were purchased from commercial suppliers. Analytical thin layer chromatography (TLC) was performed on precoated silica gel 60 F_{245}aluminium plates (Merck) with visualization under UV light. Melting points were determined on a Stuart SMP30 melting point apparatus with open capillary tubes and are uncorrected. Elemental analysis and spectral data of the compounds were performed in the Micro analytical labs, National Research Centre and Micro Analytical Laboratory Center, Faculty of Science, Cairo University, Cairo, Egypt. IR spectra (4000–400cm^{-1}) were recorded using KBr pellets in a Jasco FT/IR 300E Fourier transform infrared spectrophotometer on a Perkin Elmer FT-IR 1650(spectrophotometer).^{1}HNMR and ^{13}CNMR spectra were recorded at 500 (125) MHz, 400 (100) MHz and 300 (75) MHz on Jeol EX-, Bruker and Murcury instruments, respectively using DMSO-d_6 as a solvent. Coupling constants are reported in Hertz (Hz).Low resolution electron impact mass spectra (EI-LRMS) were recorded at 70 eV on a Finnigan SSQ 7000 instrument. The intensities are reported as percentages relative to the base peak (I = 100%).Chemical shifts are given in parts per million (ppm) relative to TMS as internal standards.

4.1. *Chemistry*

4.1.1. *General procedure for the synthesis of 4a,b* [28,31]

A solution of furfural (**1a**) (4.51 g, 47 mmol) or 5-methylfurfural (**1b**) (5.17 g, 47 mmol) in methanol (75 ml) was stirred for 10 min followed by addition of saturated solution of $Na_2S_2O_5$ (10 ml). The mixture was stirred at r.t. for 15 min followed by cooling in deep fridge overnight. Precipitated furfural bisulfite adduct **2a,b** was filtered and dried. A solution of 1,2-phenylenediamine (**3**) (4.10 g, 38 mmol), and the furfural bisulfite adduct (7.60 g, 38 mmol) or 5-methylfurfural bisulfite adduct(8.13 g, 38 mmol) in DMF (40 ml) and the mixture was stirred under reflux for 4 h. The reaction mixture was poured onto ice / water (200 ml) to give the corresponding crude product which was collected by filtration and further purified by recrystalization from methanol.

4.1.1.1 ***2-(Furan-2-yl)-1H-benzo[d]imidazole (4a)***[28,31]

Buff microcrystals; yield 80% (5.59 g); mp 285-287 °C (lit.mp:285-287 °C); R_f = 0.57 (petroleum ether /EtOAc = 2:1); IR (KBr): $\tilde{\nu}$ 3442, 3059, 1628, 1520; ^{1}H-NMR (DMSO-d_6, 500 MHz):δ_H 6.73 (dd, *J* = 3.3, 1.8 Hz, 1H), 7.18-7.23 (m, 3H), 7.53-7.58 (m, 2H), 7.93 (dd,*J* = 2.7 Hz, 1.8 Hz, 1H), 12.88 (br s, 1H); ^{13}C-NMR (DMSO-d_6, 125 MHz): δ_C 111.1, 112.9, 115.7, 115.8, 122.7, 123.4, 123.5, 144.2, 145.4, 145.6, 146.1; Anal. Calcd for $C_{11}H_8N_2O$: C, 71.73; H, 4.38; N, 15.21. Found: C, 71.69; H, 4.11; N, 15.45.

4.1.1.2. ***2-(5-Methylfuran-2-yl)-1H-benzo[d]imidazole (4b)*** [28]

Buff microcrystals; yield 85% (6.35 g); mp 272-274 °C (lit.mp: 275-277 °C); R_f = 0.71 (petroleum ether /EtOAc = 2:1); IR (KBr): $\tilde{\nu}$3423, 3050, 2950, 1631, 1505;^{1}H-NMR (DMSO-d_6, 300 MHz): δ_H 2.39 (s, 3H), 6.32 (d, *J* = 2.7 Hz, 1H), 7.08 (d, *J* = 3.0 Hz, 1H), 7.15-7.19 (m, 2H), 7.54-7.56 (m, 2H), 13.14 (br s, 1H); ^{13}C-NMR (DMSO-d_6, 75 MHz): δ_C 13.5, 108.6, 111.6, 122.1, 143.9, 144.1, 153.8; Anal. Calcd for $C_{12}H_{10}N_2O$: C, 72.71; H, 5.08; N, 14.13. Found: C, 72.55; H, 4.87; N, 14.48.

4.1.2. ***General procedure for the synthesis of 5a,b*** [28]

Ethyl bromoacetate (1.08 g, 6.5 mmol) was added dropwise to a suspension of **4a** (1.19 g, 6.5 mmol) or **4b** (1.29 g, 6.5 mmol) and anhydrous K_2CO_3 (0.90 g, 6.5 mmol) in dry acetone (20 ml). The mixture was stirred under reflux for 8 h. The mixture was then poured onto ice / water (100 ml), and the resulting precipitate was collected by filtration and recrystallized from ethanol to give the corresponding derivative **5a** or **5b**.

4.1.2.1. ***Ethyl 2-(2-(furan-2-yl)-1H-benzo[d]imidazol-1-yl)acetate (5a)*** [28]

Gray microcrystals; yield 82% (1.43 g); mp151-153 °C (lit.mp: 150-152 °C); R_f = 0.62 (petroleum ether /EtOAc = 1:1); ^{1}H-NMR (DMSO-d_6, 400 MHz): δ_H 1.19 (t, *J* = 7.0 Hz, 3H), 4.17 (q, *J* = 7.0 Hz, 2H), 5.45 (s, 2H, CH_2), 6.74 (t, *J* = 2.8 Hz, 1H), 7.21-7.29 (m, 3H), 7.67-7.69 (m, 2H), 7.80-7.94 (m, 1H); ^{13}C-NMR (DMSO-d_6, 100 MHz): δ_C 14.5, 44.6, 61.7, 110.8, 112.6, 112.8, 119.4, 123.0, 123.3, 136.3, 142.8, 144.3, 145.6, 169.6; Anal. Calcd for $C_{15}H_{14}N_2O_3$: C, 66.66; H, 5.22; N, 10.36. Found: C, 66.35; H, 5.50; N, 10.12.

4.1.2.2. ***Ethyl 2-(2-(5-methylfuran-2-yl)-1H-benzo[d]imidazol-1-yl)acetate (5b)***[28]

Gray microcrystals; yield 78% (1.44 g); mp 90-92 °C (lit.mp 88-90 °C); R_f = 0.50 (petroleum ether /EtOAc 1:1); ^{1}H-NMR (DMSO-d_6, 300 MHz): δ_H 1.19 (t, J = 7.0 Hz, 3H), 2.35 (s, 3H), 4.18 (q, J = 7.0 Hz, 2H), 5.41 (s, 2H), 6.35 (t, J = 2.8 Hz, 1H), 7.21 (t, J = 2.6 Hz, 1H), 7.27-7.29 (m, 2H), 7.67-7.69 (m, 2H); ^{13}C-NMR (DMSO-d_6, 75 MHz): δ_C 13.2, 14.0, 46.0, 52.3, 108.4, 110.1, 113.4, 118.7, 122.4, 135.8, 142.3, 143.3, 154.0, 169.0; Anal. Calcd for $C_{16}H_{16}N_2O_3$: C, 67.59; H, 5.67; N, 9.85. Found: C, 67.81; H, 6.01; N, 10.10.

4.1.3. *General procedure for the synthesis of 6a,b*

Methyl bromoacetate (0.99 g, 6.5 mmol) was added dropwise to a suspension of **4a** (1.19 g, 6.5 mmol) or **4b** (1.29 g, 6.5 mmol) and anhydrous K_2CO_3 (0.90 g, 6.5 mmol) in dry acetone (20 ml). The mixture was stirred under reflux for 8 h. The mixture was then poured onto ice / water (100 ml), and the resulting precipitate was collected by filtration and recrystallized from ethanol to give **6a** or **6b**.

4.1.3.1. *Methyl 2-(2-(furan-2-yl)-1H-benzo[d]imidazol-1-yl)acetate (6a)*

Buff microcrystals; yield 79% (1.30 g); mp 90-92 °C; R_f = 0.65 (petroleum ether /EtOAc 1:1); IR (KBr): $\tilde{\nu}$ 3046, 2954, 1745, 1612, 1509; ^{1}H-NMR (DMSO-d_6, 300 MHz): δ_H 3.71 (s, 3H), 5.45 (s, 2H), 6.74 (t, J = 2.4 Hz, 1H), 7.19 (dd, J = 3.3, 1.8 Hz, 1H), 7.26-7.28 (m, 2H), 7.64-7.68 (m, 2H), 7.91-7.94 (m, 1H); ^{13}C-NMR (DMSO-d_6, 75 MHz): δ_C 46.4, 53.0, 110.9, 112.7, 113.0, 119.5, 123.1, 123.4, 136.4, 142.9, 144.4, 145.6, 169.5;Anal. Calcd for: $C_{14}H_{12}N_2O_3$: C, 65.62; H, 4.72; N, 10.93. Found: C, 65.38; H, 4.56; N, 11.28.

4.1.3.2. *Methyl 2-(2-(5-methylfuran-2-yl)-1H-benzo[d]imidazol-1-yl)acetate (6b)*

Buff microcrystals; yield 75% (1.32 g); mp 110-112 °C; R_f = 0.65 (petroleum ether /EtOAc 1:1); IR (KBr) $\tilde{\nu}$ 3041, 2953, 1752, 1611, 1559; ^{1}H-NMR (DMSO-d_6, 300 MHz): δ_H 2.37 (s, 3H), 3.73 (s, 3H), 5.41 (s, 2H), 6.35 (d, J = 4.2 Hz, 1H), 7.19 (d, J = 3.3 Hz, 1H), 7.24-7.27 (m, 2H), 7.63-7.66 (m, 2H); ^{13}C-NMR (DMSO-d_6, 75 MHz): δ_C 13.2, 45.9, 52.3, 108.4, 110.1, 113.4, 118.7, 122.4, 135.7, 142.4, 143.9, 154.1, 169.0;Anal. Calcd for: $C_{15}H_{14}N_2O_3$: C, 66.66; H, 5.22; N, 10.36. Found: C, 66.42; H, 4.99; N, 10.11.

4.1.4. *General procedure for the synthesis of 7a,b*

A suspension of **6a** (0.51 g, 2 mmol) or **6b** (0.54 g, 2 mmol) and anhydrous K_2CO_3 (0.28 g, 2 mmol) in methanol (30 ml) was refluxed for 4 h. The mixture was filtered, the filterate was collected and evaporated under vacuum and the precipitated product was collected, washed and recrysallized from ethanol to give **7a** and **7b**, respectively.

4.1.4.1. ***2-(2-(Furan-2-yl)-1H-benzo[d]imidazol-1-yl)acetic acid (7a)***

Colorless microcrystals; yield 75% (0.36 g); mp 278-280 °C; R_f = 0.58 (petroleum ether / EtOAc 1:1); IR (KBr) $\tilde{\nu}$ 3430, 3010, 2923,1704, 1621, 1558; ^{1}H-NMR (DMSO-d_6, 400 MHz): δ_H 5.34 (s, 2H), 6.75 (t, J = 2.6 Hz, 1H), 7.20-7.30 (m, 3H), 7.65-7.96 (m, 2H), 7.95-7.96 (m, 1H), 13.29 (br s, 1H);^{13}C-NMR (DMSO-d_6, 100 MHz): δ_C 46.0, 110.3, 112.1, 112.3, 118.9, 122.4, 122.8, 135.9, 142.3, 143.9, 144.9, 145.2, 169.6; Anal. Calcd for $C_{13}H_{10}N_2O_3$: C, 64.46; H, 4.16; N, 11.56. Found: C, 64.25; H, 4.40; N, 11.15.

4.1.4.2. ***2-(2-(5-Methylfuran-2-yl)-1H-benzo[d]imidazol-1-yl)acetic acid (7b)***

Buff microcrystals; yield 78% (0.39 g); mp 258-260 °C; R_f = 0.71 (petroleum ether / EtOAc = 1:1); IR (KBr) $\tilde{\nu}$3424, 3009, 2956,1706, 1616, 1561; ^{1}H-NMR (DMSO-d_6, 300 MHz):δ_H 2.36 (s, 3H), 5.26 (s, 2H), 6.34 (d, J = 2.1 Hz, 1H), 7.06 (d, J = 3 Hz, 1H), 7.23-7.26 (m, 2H), 7.59-7.66 (m, 2H);^{13}C-NMR (DMSO-d_6, 75 MHz): δ_C 13.3, 46.2, 108.3, 110.1, 113.3, 118.6, 122.2, 122.4, 135.9, 142.3, 143.4, 144.1, 153.8, 169.7; Anal. Calcd for $C_{14}H_{12}N_2O_3$: C, 65.62; H, 4.72; N, 10.93. Found: C, 65.45; H, 4.48; N, 10.68.

4.1.5. ***General procedure for the synthesis of 8a, b*** [28]

Hydrazine hydrate (1.00 g, 20 mmol) was added dropwise to a solution of **5a** (2.70 g, 10 mmol) or **5b** (2.85 g, 10 mmol) in methanol (15 ml). The reaction mixture was refluxed for 4 h. After cooling to r.t., the reaction mixture was concentrated by evaporation under reduced pressure. The crude product was filtered, washed with small portions of cold ethanol and cold water repeatedly. Further crystallization from ethanol afforded **8a** and **8b**, respectively.

4.1.5.1. ***2-(2-(Furan-2-yl)-1H-benzo[d]imidazol-1-yl)acetohydrazide (8a)*** [28]

Buff microcrystals; yield 88% (2.25 g); mp 239-241 °C (lit.mp 240-242 °C); R_f = 0.70 (petroleum ether /EtOAc = 1:1); IR (KBr): $\tilde{\nu}$ 3325, 3254, 3131, 1650, 1611, 1510; ^{1}H-NMR (DMSO-d_6, 300

MHz): δ_H 4.32 (br s, 2H),5.12 (s, 2H), 6.72 (t, *J* = 3.0 Hz, 1H), 7.16 (dd, *J* = 3.6, 1.8 Hz,1H), 7.2-7.23 (m, 2H), 7.49-7.62 (m, 2H), 7.91-7.92 (m, 1H), 9.49 (br s, 1H*)*; ^{13}C-NMR (DMSO-d_6, 75 MHz): δ_C 46.11, 110.7, 112.9, 119.3, 122.5, 123.1, 136.6, 142.9, 144.7, 145.2, 145.8, 166.7, 170.8; Anal. Calcd for $C_{13}H_{12}N_4O_2$: C, 60.93; H, 4.72; N, 21.86. Found: C, 60.67; H, 5.0; N, 21.55.

4.1.5.2. ***2-(2-(5-Methylfuran-2-yl)-1H-benzo[d]imidazol-1-yl)acetohydrazide (8b)*** [28]

Buff microcrystals; yield 90% (2.43 g); mp 244-246 °C (lit.mp 246-248 °C); R_f = 0.57 (petroleum ether / EtOAc = 1:1); IR (KBr) $\tilde{\nu}$ 3348, 3252, 3131, 1660, 1612, 1510; ^{1}H-NMR (DMSO-d_6, 300 MHz):δ_H 2.35 (s, 3H), 4.30 (br s, 2H),5.00 (s, 2H), 6.30 (d, *J* = 3.0 Hz, 1H), 7.00 (d, *J* = 3.0 Hz,1H), 7.20-7.25 (m, 2H), 7.57-7.60 (m, 2H); Anal. Calcd for $C_{14}H_{14}N_4O_2$: C, 62.21; H, 5.22; N, 20.73. Found: C, 62.45; H, 5.47; N, 21.00.

4.1.6. ***1-((5-(Trichloromethyl)-1,3,4-oxadiazol-2-yl)methyl)-2-(furan-2-yl)-1H-benzo[d]imid-azole (9a)***

A solution of **8a** (2.50 g, 10 mmol) and trichloroacetic acid (1.60 g, 10 mmol) in phosphorus oxychloride (15 ml) was refluxed for 20 h, followed by cooling to r.t. The mixture was poured onto ice / water (50 ml) to give the precipitated crude product which was collected by filtration. Further purification by crystallization from methanol afforded **9a** as buff microcrystals; yield 65% (2.47 g); mp 270-272 °C; R_f = 0.67 (petroleum ether / EtOAc = 2:1); IR (KBr), $\tilde{\nu}$ 3081, 2930, 1632, 1527;^{1}H-NMR (DMSO-d_6, 400 MHz): δ_H 5.42 (s, 2H), 6.81 (t, *J* = 3.2 Hz, 1H), 7.34-7.39 (m, 3H), 7.69-7.79 (m, 2H), 8.06 (dd, *J* = 3.3, 1.8 Hz, 1H); ^{13}C-NMR (DMSO-d_6, 100 MHz): δ_C47.0, 91.5, 112.4, 113.6, 116.4, 117.9, 125.5, 125.7, 134.6, 135.2, 140.7, 142.2, 148.3, 161.5, 165.6; Anal. Calcd for $C_{15}H_9Cl_3N_4O_2$: C, 64.96; H, 2.36; N, 14.60. Found: C, 64.69; H, 2.70; N, 14.29.

4.1.7. ***1-((1,3,4-Oxadiazol-2-yl)methyl)-2-(5-methylfuran-2-yl)-1H-benzo[d]imidazole (9b)***

A solution of **8b** (2.70 g, 10 mmol) and formic acid (0.50 g, 10 mmol) in phosphorus oxychloride (15 ml) was refluxed for 20 h, followed by cooling to r.t. The mixture was poured onto ice / water (50 ml) to give the precipitated crude product which was collected by filtration and further purified by recrystalization from methanol to afford **9b** as buff microcrystals; yield 70% (1.96 g); mp 260-262 °C; R_f = 0.54 (petroleum ether /EtOAc = 2:1); IR (KBr)$\tilde{\nu}$ 3060, 2930, 1618, 1514;^{1}H-NMR (DMSO-d_6, 300 MHz): δ_H 2.39 (s, 3H), 5.12 (s, 2H), 6.33 (d, *J* = 2.4 Hz, 1H), 7.04 (d, *J* = 3.3 Hz, 1H), 7.21-

7.26 (m, 3H), 7.56-7.63 (m, 2H); ^{13}C-NMR (DMSO-d_6, 75 MHz): δ_C 12.4,45.6, 108.2, 110.3, 113.4, 118.6, 122.1, 122.3, 136.1, 134.6, 142.4, 143.1, 144.3, 153.9, 166.3; Anal. Calcd for $C_{15}H_{12}N_4O_2$: C, 64.28; H, 4.32; N, 19.99; Cl, 27.73. Found: C, 64.53; H, 4.01; N, 19.65; Cl, 27.55.

4.1.8. ***General procedure for the synthesis of 10a,b***

A solution of **8a** (2.56 g, 10 mmol) or **8b** (2.70 g, 10 mmol), 2-chlorobenzaldehyde (1.40 g, 10 mmol) and 10% NaOH (1 ml) in ethanol (20 ml) was stirred at r.t. for 4 h. The mixture was kept at r.t. overnight and the formed crude product was collected by filtration and further purified by recrystalization from methanol to give **10a** and **10b**, respectively.

4.1.8.1.*1-(1-(2-Chlorophenyl)-3-(2-(furan-2-yl)-1H-benzo[d]imidazol-1-yl)prop-1-en-2-yl)hydrazine (10a)*

Brown microcrystals; yield 80% (3.02 g); mp 220-222 °C; R_f = 0.50 (petroleum ether / EtOAc = 2:1); IR (KBr): $\tilde{\nu}$ 3407, 2995, 1650, 1610, 1509; ^{1}H-NMR (DMSO-d_6, 300 MHz): δ_H 5.83 (s, 2H), 6.80 (t, J = 2.5 Hz, 1H), 7.33-7.39 (m, 1H), 7.45-7.49 (m, 3H), 7.53-7.59 (m, 2H), 7.74-7.80 (m, 3H), 8.00-8.01 (m,1H), 8.46 (d, J = 7.8, 1H), 8.98 (s, 1H), 9.81 (br s, 1H); ^{13}C-NMR (DMSO-d_6, 75 MHz): δ_C 44.4, 110.9, 113.0, 113.9, 119.3, 123.8, 124.1, 128.0, 128.8, 130.2, 130.5, 131.2, 133.7, 134.8, 136.5, 144.4, 144.6, 146.2, 150.2, 161.7; Anal. Calcd for $C_{20}H_{15}ClN_4O_2$: C, 63.41; H, 3.99; N, 14.79; Cl, 9.36. Found: C, 63.23; H, 4.25; N, 15.01; Cl, 9.16.

4.1.8.2. ***1-(1-(2-Chlorophenyl)-3-(2-(5-methylfuran-2-yl)-1H-benzo[d]imidazol-1-yl)prop-1-en-2-yl)hydrazine (10b)***

Buff microcrystals; yield 85% (3.33 g); mp 230-232 °C; R_f = 0.70 (petroleum ether / EtOAc = 2:1); IR (KBr): $\tilde{\nu}$ 3396, 3029, 2900, 1694, 1630, 1513;^{1}H-NMR (DMSO-d_6, 300 MHz): δ_H 2.4 (s, 3H), 5.98 (s, 2H), 6.50 (d, J = 2.7 Hz, 1H), 7.33-7.39 (m, 3H), 7.45-7.49 (m, 3H), 7.53-7.59 (m, 2H), 8.12-8.15 (m,1H), 8.60 (s, 1H), 12.3 (br s, 1H); ^{13}C-NMR (DMSO-d_6, 75 MHz): δ_C 13.3, 45.8, 108.5, 110.5, 113.7, 118.2, 122.5, 127.1, 127.6, 129.9, 131.4, 133.0, 136.1, 140.2, 143.2, 141.4, 143.8, 154.2, 168.7; Anal. Calcd for $C_{21}H_{17}ClN_4O_2$: C, 64.21; H, 4.36; N, 14.26; Cl, 9.36. Found: C, 63.95; H, 4.19; N, 14.56; Cl, 9.19.

4.1.9. ***2-(2-(Furan-2-yl)-1H-benzo[d]imidazol-1-yl)acetonitrile (11)***

Chloroacetonitrile (4.20 g, 56 mmol) was added dropwise to a suspension of **4a** (10.30 g, 56 mmol) and anhydrous K_2CO_3 (7.73 g, 56 mmol) in acetone (30 ml). The mixture was refluxed for 8 h, followed by addition of ice / water (200 ml). The precipitated crude product was filtered and further purified by recrystallization from methanol to give **11** as gray microcrystals; yield 87% (10.81 g); mp140-142 °C; R_f = (methylene chloride / petroleum ether = 2:1); IR (KBr) $\tilde{\nu}$ 3052, 2917, 2194, 1611, 1511; ^{1}H-NMR (DMSO-d_6, 500 MHz): δ_H 5.80 (s, 2H), 6.79 (t, J = 3.3 Hz, 1H), 7.29-7.35 (m, 3H), 7.52 (d, J = 7.6 Hz, 1H), 7.77 (d, J = 7.6 Hz, 1H), 8.04 (dd, J = 3.3, J = 1.5 Hz, 1H); ^{13}C-NMR (DMSO-d_6, 125 MHz): δ_C34.0, 110.8, 113.0, 113.9, 116.7, 120.0, 123.9, 124.1, 135.3, 142.9, 143.6, 144.6, 146.2; Anal. Calcd for $C_{13}H_9N_3O$: C, 69.95; H, 4.06; N, 18.82. Found C, 69.74; H, 3.75; N, 19.13.

4.1.10. *2-(2-(Furan-2-yl)-1H-benzo[d]imidazol-1-yl)acetimidohydrazide (12)*

Hydrazine hydrate (1.00 g, 20 mmol) was added dropwise to a solution of **11** (2.23 g, 10 mmol) in methanol (15 ml). The reaction mixture was refluxed for 4 h. After cooling to r.t., the reaction mixture was concentrated to one third by evaporation of the solvent under reduced pressure. The crude product was collected by filtration, washed with small portions of cold ethanol and cold water repeatedly then left to dry. The crude product was further purified by recrystallization from ethanol to give **12** as buff microcrystals; yield 88% (2.24 g); mp 240-242 °C; R_f = 0.65 (petroleum ether / EtOAc 1:1);IR (KBr) $\tilde{\nu}$ 3325, 3254, 3131, 2930, 1611, 1510; ^{1}H-NMR (DMSO-d_6, 300 MHz): δ_H 4.59 (br s, 2H), 5.04 (s, 2H, CH_2), 5.44 (br s, 1H), 6.69 (t, J = 1.8 Hz, 1H), 7.16-7.27 (m, 3H), 7.46-7.4 8 (m, 2H), 7.90 (dd, J = 2.1, 1.2 Hz, 1H); ^{13}C-NMR (DMSO-d_6, 75 MHz): δ_C 46.2, 111.4, 112.6, 113.0, 119.4, 122.6, 123.0, 136.7, 143.0, 143.8, 144.8, 145.5; Anal. Calcd for $C_{13}H_{13}N_5O$: C, 61.17; H, 5.13; N, 27.43. Found: C, 61.45; H, 5.52; N, 27.15.

4.1.11. *5-((-2-(Furan-2-yl)-1H-benzo[d]imidazol-1-yl)methyl)-1,3,4-thiadiazole-2(3H)-thione (13)*

Carbon disulfide (0.75 ml, 10 mmol) was added dropwise to an ice/cooled solution of acid hydrazide **12** (1.28 g, 5 mmol) and KOH (0.66 g, 5 mmol) in ethanol (10 ml). The reaction mixture was stirred at r.t. for 2 h. After dilution with ethanol, the formed precipitate was filtered and washed twice with ether. A solution of the formed intermediate (1.47 g, 4 mmol) in 10% KOH (10 ml) was refluxed for 10 h, followed by cooling to r.t. and acidification with conc. HCl (2 ml). The crude product was filtered, washed with water, dried and crystallized from DMF to afford **13** as buff microcrystals; yield

74% (1.16 g); mp 260-262 °C; R_f = 0.68 (petroleum ether /EtOAc = 1:1); IR (KBr) $\tilde{\nu}$ 3434, 3010, 2944, 1610, 1510, 1260, 648; ^{1}H-NMR (DMSO-d_6, 300 MHz): δ_H 5.97 (s, 2H, CH_2), 6.75 (dd, J = 2.1, 1.8 Hz, 1H), 7.28-7.34 (m, 3H), 7.68-7.70 (m, 2H), 7.99-8.00 (m, 1H), 14.20 (br s, 1H);^{13}C-NMR (DMSO-d_6, 75 MHz): δ_C 42.4, 111.2, 113.0, 114.0, 119.5, 123.8, 124.0, 135.6, 142.2, 143.7, 144.5, 146.1, 159.2, 189.1; Anal. Calcd for $C_{14}H_{10}N_4OS_2$: C, 53.49; H, 3.21; N, 17.82; S, 20.40. Found: C, 53.83; H, 3.52; N, 17.53; S, 20.18.

4.1.12.Ethyl-2-((5-((2-(furan-2-yl)-1H-benzo[d]imidazol-1-yl)methyl)-1,3,4-thiadiazol-2-yl)thio)acetate (14)

A suspension of **13** (0.63 g, 2 mmol) and anhydrous K_2CO_3 (0.28 g, 2 mmol) in dry acetone (30 ml) was stirred at r.t. for 0.5 h, followed by addition of ethyl bromoacetate (0.33 g, 2 mmol). The reaction mixture was refluxed for 4 h. After cooling to r.t., ice / water (100 ml) was added and the precipitated product was filtered and recrysallized from ethanol to give **14** as buff microcrystals; yield 74% (0.59 g); mp 279-281 °C; R_f = 0.58 (petroleum ether / EtOAc = 1:3); IR (KBr) $\tilde{\nu}$ 3114, 2973, 1735, 1613, 1510; ^{1}H-NMR (DMSO-d_6, 300 MHz): δ_H 1.07 (t, J = 7.0 Hz, 3H), 4.06 (q, J = 7.0 Hz, 2H), 4.18 (s, 2H), 6.21 (s, 2H), 6.75 (dd, J = 3.3, 1.5 Hz, 1H), 7.26-7.33 (m, 3H), 7.68-7.69 (m, 2H), 7.96 (dd, J = 3.3, 1.8 Hz, 1H); ^{13}C-NMR (DMSO-d_6, 75 MHz): δ_C 13.8, 35.1, 42.9, 61.3, 110.5, 112.3, 113.0, 119.2, 123.0, 123.2, 135.1, 142.5, 143.3, 144.4, 145.2, 165.7, 165.9, 167.7; Anal. Calcd for $C_{18}H_{16}N_4O_3S_2$: C, 53.98; H, 4.03; N, 13.99; S, 16.01. Found: C, 53.64; H, 4.24; N, 13.65; S, 16.35.

4.1.13.2-((5-((2-(Furan-2-yl)-1H-benzo[d]imidazol-1-yl)methyl)-1,3,4-thiadiazol-2-yl)thio)acetohydrazide (15)

A solution of **14** (4.00 g, 10 mmol) and hydrazine hydrate (1.00 g, 20 mmol) in methanol (15 ml) was refluxed for 4 h, followed by cooling to r.t. Excess solvent was evaporated under vacuum and the crude product was separated by filtration. The product was purified by recrystallization from ethanol to give **15** as buff microcrystals; yield 85% (3.30 g); mp 250-252 °C; R_f = 0.65 (petroleum ether / EtOAc = 1:1); IR (KBr) $\tilde{\nu}$ 3481, 3268, 3051, 2951, 1751, 1629, 1565, 660; ^{1}H-NMR (DMSO-d_6, 400 MHz): δ_H 4.34 (s, 2H), 4.69 (br s, 2H), 5.14 (s, 2H), 6.74 (t, J = 2.5 Hz, 1H), 7.18 (dd, J = 3.3, 1.7 Hz,1H), 7.24-7.29 (m, 2H), 7.52 (d, J = 8.5 Hz, 1H), 7.54 (d, J = 8.6 Hz, 1H), 7.93-7.95 (m, 1H), 9.53 (br s, 1H);^{13}C-NMR (DMSO-d_6, 100 MHz): δ_C 43.3, 43.6, 111.2, 112.8, 113.5, 119.7, 123.3,

135.6, 143.0, 143.8, 144.9, 145.7, 153.6, 155.4, 166.1, 169.9; Anal. Calcd for $C_{16}H_{14}N_6O_2S_2$: C, 49.73; H, 3.65; N, 21.75; S, 16.59. Found: C, 49.55; H, 3.86; N, 21.93; S, 16.71.

4.1.14. 2-(2-(Furan-2-yl)-1H-benzo[d]imidazol-1-yl)-2-(4-oxo-3-phenylthiazolidin-2-ylidene)acetonitrile (16)

A solution of compound **11** (0.89 g, 4 mmol) and KOH (0.22 g, 4 mmol) in DMF (10 ml) was stirred for 10 min, followed by addition of phenyl isothiocyanate (0.54 ml, 4 mmol) and the mixture was stirred for additional 30 min. Ethyl bromoacetate (0.66 g, 4 mmol) was added and stirring was continued for 2 h. The mixture was poured onto ice / water (200 ml) and the precipitated crude product was collected by filtration. Further purification by recrystallization from methanol afforded **16** as buff microcrystals; yield 82% (1.30 g); mp 240-242 °C; R_f = 0.47 (petroleum ether / EtOAc = 2:1); IR (KBr) $\tilde{\nu}$ 3049, 2930, 2197, 1664, 1636, 1511; ^{1}H-NMR (DMSO-d_6, 300 MHz):δ_H4.16 (s, 2H), 6.86-6.89 (m, 2H), 7.08-7.13 (m, 2H), 7.31-7.36 (m, 3H), 7.39-7.40 (m, 2H), 7.40-7.52 (m, 2H), 7.53-7.55 (m, 1H); ^{13}C-NMR (DMSO-d_6, 75 MHz): δ_C32.8, 120.6, 124.2, 128.4, 128.9, 129.2, 135.3, 148.1, 155.8, 171.6; Anal. Calcd for $C_{22}H_{14}N_4O_2S$: C, 66.32; H, 3.54; N, 14.06; S, 8.05. Found: C, 66.02; H, 3.81; N, 13.76;S, 8.33.

4.1.15. 2-((2-(Furan-2-yl)-1H-benzo[d]imidazol-1-yl)methylene)thiazolidin-4-one (17)

Thioglycolic acid (2.73 g, 30 mmol) was added dropwiseto a solution of **11** (6.69 g, 30 mmol) in ethanol (30 ml). The mixture was stirred under reflux for 8 h. The reaction mixture was poured onto ice / water and the precipitated crude product was collected by filtration. Further purification by recrystallization from ethanol afforded **17** as gray microcrystals; yield 74% (6.62 g); mp192-194 °C; R_f = 0.62 (petroleum ether / EtOAc = 1:2); IR (KBr) $\tilde{\nu}$ 3289, 3096, 2922, 1705, 1644, 1508; ^{1}H-NMR (DMSO-d_6, 400 MHz): δ_H 3.58 (s, 1H),5.50 (d, 2H), 6.75 (dd, J = 3.3, 1.5 Hz, 1H), 7.20-7.32 (m, 3H), 7.66-7.70 (m, 2H), 7.63 (s, 1H), 8.00 (m,1H); ^{13}C-NMR (DMSO-d_6, 75MHz): δ_C 46.0, 71.5, 110.3, 112.1, 112.5, 118.9, 122.7, 131.2, 135.9, 142.3, 144.3, 145.2, 169.6; Anal. Calcd for $C_{15}H_{11}N_3O_2S$: C, 60.59; H, 3.73; N, 14.13; S, 10.78. Found: C, 60.19; H, 3.43; N, 14.43; S, 10.65.

4.1.16. 2-(2-(Furan-2-yl)-1H-benzo[d]imidazol-1-yl)acetamide (18)

Piperidine (2.55 g, 30 mmol) was added dropwise to a solution of **11** (6.69 g, 30 mmol) in ethanol (30 ml). The mixture was stirred under reflux for 8 h, the reaction mixture was poured onto ice /

water (100 ml) and the precipitated crude product was collected by filtration. Further purification by recrystallization from ethanol afforded **18** as gray microcrystals; yield 70% (5.06 g); mp179-181 °C; R_f = 0.54 (petroleum ether / EtOAc = 2:1); IR (KBr) $\tilde{\nu}$ 3354, 3052, 2938, 1681, 1611, 1511; ^{1}H-NMR (DMSO-d_6, 300 MHz): δ_H5.14 (s, 2H), 6.71 (t, J = 2.4 Hz, 1H), 7.14 (dd, J = 3.3, 1.5 Hz 1H), 7.25-7.28 (m, 2H), 7.47 (d, J = 7.2 Hz, 1H), 7.63 (d, J = 7.2 Hz, 1H), 7.75 (s, 2H), 7.85 (dd, J = 3.3, 1.5 Hz, 1H); ^{13}C-NMR (DMSO-d_6, 75MHz): δ_C 47.5, 110.9, 112.6, 112.8, 123.2, 136.8, 143.0, 144.7, 145.4, 145.76, 169.2; Anal. Calcd for $C_{13}H_{11}N_3O_2$: C, 64.72; H, 4.60; N, 17.42. Found: C, 64.39; H, 4.83; N, 17.13.

4.1.17. General procedure for the synthesis of 19a, b

Benzaldehyde (1.06 g, 10 mmol) or 2-chlorobenzaldehyde (1.40 g, 10 mmol) was added to a solution of **18** (2.40 g, 10 mmol) and 10% NaOH solution (10 ml) in ethanol (20 ml). The mixture was stirred at r.t. for 4h, then was kept overnight at r.t. The precipitated crude product was collected by filtration and further purified by recrystalization from methanol to give **19a** and **19b**, respectively.

4.1.17.1. 2-(-2-(Furan-2-yl)-1H-benzo[d]imidazol-1-yl)-3-phenylacrylamide (19a)

Brown microcrystals; yield 87% (2.85 g); mp 225-227 °C; R_f = 0.49 (petroleum ether /EtOAc = 2:1); IR (KBr) $\tilde{\nu}$ 3320, 3066, 1688, 1617, 1511;^{1}H-NMR (DMSO-d_6, 300 MHz): δ_H 6.64 (m, 1H), 6.82-6.85 (m, 1H), 7.02-7.07 (m, 2H), 7.16-7.25 (m, 5H), 7.49 (br s, 2H), 7.71-7.74 (m, 2H), 7.85-7.86 (m, 1H), 7.99 (s, 1H); ^{13}C-NMR (DMSO-d_6, 75 MHz): δ_C 109.8, 112.0, 119.3, 122.8, 123.3, 127.2, 128.1, 128.6, 129.5, 130.5, 130.9, 131.0, 131.1, 133.2, 134.8, 142.7, 143.6, 144.4, 145.2, 164.4; Anal. Calcd for $C_{20}H_{15}N_3O_2$: C, 72.94; H, 4.59; N, 12.76. Found: C, 72.65; H, 4.27; N, 12.39.

4.1.17.2. 3-(2-Chlorophenyl)-2-(-2-(furan-2-yl)-1H-benzo[d]imidazol-1-yl)acrylamide (19b)

Brown microcrystals; yield 83% (3.00 g); mp 210-212 °C; R_f = 0.47 (petroleum ether / EtOAc = 2:1); IR (KBr) $\tilde{\nu}$ 3316, 3050, 1688, 1618, 1509; ^{1}H-NMR (DMSO-d_6, 300 MHz): δ_H 6.43 (dd, J = 3.3, 1.5 Hz, 1H), 6.68-6.91 (m, 1H), 6.91-7.06 (m, 3H), 7.19-7.22 (m, 3H), 7.44-7.47 (d, J = 8.1 Hz, 1H), 7.64-7.67 (d, J = 7.2 Hz, 1H), 7.89-7.91 (m, 1H), 8.01 (br s, 2H), 8.06 (s, 1H); ^{13}C-NMR (DMSO-d_6, 75 MHz): δ_C 109.8, 112.0, 119.3, 122.7, 123.3, 127.2, 128.1, 128.6, 129.5, 130.5, 130.9, 131.1, 133.2, 134.8, 142.7, 143.6, 144.4, 145.2, 164.4; Anal. Calcd for $C_{20}H_{14}ClN_3O_2$: C, 66.03; H, 3.88; N, 11.55; Cl, 9.75. Found: C, 66.33; H, 3.62; N, 11.95; Cl, 9.51.

4.1.18. 2-(5-(Morpholinomethyl)furan-2-yl)-1H-benzo[d]imidazole (20)

A solution of **4a** (1.84 g, 10 mmol) and paraformaldehyde (1 g) in ethanol (20 ml) was stirred at r.t. for 5 min, followed by the addition of conc. HCl (1 ml) and morpholine (1.04 g, 12 mmol). Stirring was continued at r.t. for 1 h followed by stirring under reflux for additional 2 h. The reaction mixture was then filtered, and the filtrate was concentrated to one third its original volume and kept in refrigerator overnight. The precipitated crude product was collected by filtration and dried. The crude product was purified by recrystallization from ethanol to give**20** as red microcrystals; yield 80% (2.26); mp> 300 °C; R_f = 0.39 (petroleum ether /EtOAc = 2:1); IR (KBr): $\tilde{\nu}$ 3423, 3069, 2855, 1633, 1568; ^{1}H-NMR (DMSO-d_6, 500 MHz): δ_H 2.56-2.58 (m, 4H), 3.31 (s, 2H), 3.68-3.70 (m, 4H), 6.56 (d, J = 2.4 Hz, 1H), 7.13 (d, J = 2.4 Hz, 1H), 7.24-7.25 (m, 2H), 7.57-7.58 (m, 2H); ^{13}C-NMR (DMSO-d_6 125 MHz): δ_C 53.3, 54.9, 66.6, 111.7, 111.9, 122.6, 144.3, 145.7, 153.7; Anal. Calcd for $C_{16}H_{17}N_3O_2$: C, 67.83; H, 6.05; N, 14.83. Found: C, 67.51; H, 6.39; N, 14.53.

4.1.19. 2-Chloro-1-(2-(furan-2-yl)-1H-benzo[d]imidazol-1-yl)ethan-1-one (21)

Chloroacetyl chloride (4.5 ml, 56.5 mmol) was added dropwise to a suspension of **4a** (10.00 g, 56.5 mmol) and anhydrous K_2CO_3 (7.70 g, 56.5 mmol) in dry acetone (30 ml). The mixture was stirred at r.t. for 8 h. The mixture was filtered, the filterate was collected and evaporated under vacuum to give **21**) as gray powder; highly hygroscopic so used directly in the next reaction step without any further purification.

4.1.20. 6-(2-(Furan-2-yl)-1H-benzo[d]imidazol-1-yl)-1,6-dihydro-1,2,4-triazine-3-thiol (22)

Thiosemicarbazide (0.51 g, 5.65 mmol) was added to a suspension of freshly prepared **21** (1.50 g, 5.65 mmol), and anhydrous K_2CO_3 (0.78 g, 5.65 mmol) in dry acetone (30 ml). The mixture was stirred at r.t. for 8 h, followed by filtration. The filtrate was evaporated under reduced pressure to give the crude product which was crystallized from ethanol to give **22** as brown microcrystals, yield 70% (1.20 g); mp> 300 °C; R_f = 0.63 (petroleum ether / EtOAc = 1:1); IR (KBr): $\tilde{\nu}$ 3424, 3058, 2923, 1627, 1523; ^{1}H-NMR (DMSO-d_6, 300 MHz):δ_H1.17 (s, 1H), 2.50 (s, 2H), 6.71 (t, J= 2.7 Hz, 1H), 7.18-7.21 (m, 3H), 7.54-7.58 (m, 2H), 7.92-7.93 (m, 1H), 8.60 (br s, 1H), 13.00 (s,1H);^{13}C-NMR (DMSO-d_6, 75 MHz): δ_C 45.3, 113.0, 114.3, 115.4, 124.4, 134.2, 141.0, 141.3, 147.1, 157.7, 162.9; Anal. Calcd for $C_{14}H_{11}N_5OS$: C, 56.55; H, 3.73; N, 23.55; S, 10.78. Found: C, 56.17; H, 3.45; N, 23.18; S, 10.53.

4.1.21. 4-[2-(Furan-2-yl)-1H-benzo[d]imidazol-1-yl]-1,5-dihydro-1H-imidazol-2-imine (23)

Guanidine hydrochloride (0.54 g, 5.65 mmol) was added to a suspension of freshly prepared **21** (1.50 g, 5.65 mmol), and anhydrous K_2CO_3 (0.78 g, 5.65 mmol) in dry acetone (30 ml). The mixture was stirred at r.t. for 8 h, followed by filteration and the filtrate was evaporated under reduced pressure. The crude product was crystallized from ethanol to give **23** as brown microcrystals; yield 73% (1.12 g); mp> 300 °C; R_f = 0.60 (petroleum ether / EtOAc = 1:1); IR (KBr): $\tilde{\nu}$ 3413, 3058, 2864, 1625, 1520; ^{1}H-NMR (DMSO-d_6, 300 MHz): δ_H 2.50 (s, 2H), 3.31 (br s, 1H), 6.71 (t, J = 2.6 Hz, 1H), 7.18-7.19 (m, 3H), 7.30-7.58 (m, 2H), 7.93 (m, 1H), 12.87 (br s, 1H);^{13}C-NMR (DMSO-d_6, 75 MHz): δ_C 45.6, 110.5, 112.0, 112.5, 118.7, 120.5, 122.4, 122.7, 135.9, 142.2, 144.2, 144.6, 144.9, 166.0; Anal. Calcd for $C_{14}H_{11}N_5O$: C, 63.39; H, 4.18; N, 26.40. Found: C, 63.03; H, 4.43; N, 26.12.

4.1.22. Bis(2-(5-methylfuran-2-yl)-1H-benzo[d]imidazol-1-yl)methanone (24)

A solution of **4b** (3.94 g, 20 mmol) and diethyl carbonate (1.18 g, 10 mmol) in ethanol (5 ml) was stirred at r.t. for 4 h followed by addition of conc. HCl (2 ml). Stirring was continued for additional 1 h. The formed crude product was collected by filtration and further purified by recrystalization from methanol to give **24** as green microcrystals, yield 87% (7.36 g); mp 220-222 °C; R_f = 0.57 (petroleum ether /EtOAc = 2:1); IR (KBr): $\tilde{\nu}$ 3046, 2951, 1682, 1617, 1561;^{1}H-NMR (DMSO-d_6, 300 MHz): δ_H 2.40 (s, 6H), 6.33 (d, J = 3.3 Hz, 2H), 7.09 (d, J = 3.3 Hz, 2H), 7.18-7.19 (m, 4H), 7.52-7.53 (m, 4H); ^{13}C-NMR (DMSO-d_6, 75 MHz): δ_C 13.8, 110.4, 113.6, 119.9, 125.8, 130.9, 136.6, 139.3, 158.7, 160.8; Anal. Calcd for $C_{25}H_{18}N_4O_3$: C, 71.08; H, 4.29; N, 13.26. Found: C, 71.43; H, 4.53; N, 12.92.

4.1.23. 1,2-Bis[2-(5-methylfuran-2-yl)-1H-benzo[d]imidazol-1-yl]ethane-1,2-dione (25)

A solution of **4b** (3.94 g, 20 mmol) and diethyl oxalate (1.46 g, 10 mmol) in ethanol (5 ml) was stirred at r.t. for 4 h, followed by the addition of conc. HCl (2 ml). Stirring was continued for additional 1 h. The formed crude product was collected by filtration and further purified by recrystalization from methanol to give **25**as green microcrystals; yield 80% (7.20 g); mp 245-247 °C; R_f = 0.57 (petroleum ether /EtOAc = 2:1); IR (KBr): $\tilde{\nu}$ 3042, 2920, 1694, 1646, 1509; ^{1}H-NMR (DMSO-d_6, 300 MHz): δ_H 2.34 (s, 6H), 6.32 (d, J = 3.3 Hz, 2H), 7.10 (d, J = 3.3 Hz, 2H), 7.16-7.21 (m, 4H), 7.53-7.57 (m, 4H); ^{13}C-NMR (DMSO-d_6, 75 MHz): δ_C 13.4, 108.9, 113.1, 114.6, 122.8,

131.6, 137.3, 142.4, 143.0, 154.7, 166.8; Anal. Calcd for $C_{26}H_{18}N_4O_4$: C, 69.33; H, 4.03; N, 12.44. Found: C, 69.57; H, 3.75; N, 12.78.

4.2.Biological studies

4.2.1. Cytotoxicity against human breast cancer (MCF-7) and hepatocellular carcinoma (HepG2) cell lines

The cytotoxicity of the synthesized compounds against MCF-7 and HepG2 cancer cell lines were performed in the National Cancer Institute, Cancer Biology Department, Cairo University, Egyptutilizing SRB assay [32,33]. Cells were plated in 96 multi-well plate (96 cells/well) for 24 h before treatment with the compounds to allow attachment of cell to wall of the plate. Different concentrations of the compound under test (0.0, 5.0, 12.5, 25.0 and 50 mg/ml) were added to the cell monolayer. Monolayer cells were incubated with the compounds for 48 h at 37 °C and in atmosphere of 5% CO_2. After 48 h, cells were fixed, washed and stained with sulforhodamine B stain. Excess stain was washed with acetic acid and attached stain was recovered with Tris EDTA buffer. Color intensity was measured in an ELISA reader. The relation between surviving fraction and drug concentration was plotted to get the survival curve of tumor cell line after the specified compound.

4.2.2. Studying the effect of synthesized compounds on the level of VEGFR-2 in MCF-7cell line

The effect of the synthesized compounds on the level of human vascular endothelial growth factor receptor-2 (VEGFR-2) was determined utilizing human breast cancer MCF7 cell line obtained from the American Type Culture Collection (Rockville, MD, USA). The cells in culture medium were treated with 20 µl of the cytotoxic IC_{50} values of the compounds or the standard reference drugs dissolved in DMSO, then incubated for 24 h at 37 °C, in a humidified 5% CO_2 atmosphere. The cells were harvested and homogenates were prepared in saline using a tight pestle homogenizer until complete cell disruption. The kit uses a double-antibody sandwich enzyme-linked immunosorbent assay (ELISA) to assay the level of human VEGFR-2 in samples. A monoclonal antibody for VEGFR-2 has been pre-coated onto 96-well plates. Standard and test samples are added to the wells. Abiotinylated detection polyclonal antibody from goat specific for VEGFR-2 is added subsequently and then followed by washing with PBS buffer. Avidin-Biotin-Peroxidase complex was added and unbound conjugates were washed away with PBS buffer. HRP substrate TMB was used to visualize

HRP enzymatic reaction. TMB was catalyzed by HRP to produce a blue color product that changed into yellow after adding acidic stop solution. The density of the yellow color is proportional to the human VEGFR-2 amount of sample captured in the plate. The chroma of the yellow color and the concentration of the human VEGFR-2 of the sample were positively correlated and the optical density was determined at 451 nm. The level of human VEGFR-2 in samples was calculated (ng/ml) as duplicate determinations from the standard curve. Percent inhibition was calculated by the comparison of the tested compounds treated to control cancer cells. The obtained data were compared with Sorafenib as standard inhibitor for VEGFR-2.

4.2.3. In vitro effect of the synthesized compounds on VEGFR-2

Compounds **10a**, **10b**, **15** were evaluated for their *in vitro* inhibitory activity against Human VEGFR-2 using ELISA (Enzyme-Linked Immunosorbent Assay) kit according to manufacturer's instructions (Ray Biotech). This assay employs an antibody specific for human VEGFR-2 coated on a 96-well plate. Standards and samples are pipetted into the wells and incubated over night at 4°C with gentle shaking. The wells are washed and biotinylated antibody is added followed by incubation for one hour at room temperature. After washing away unbound biotinylated antibody, HRP-conjugated streptavidin is pipetted to the wells. The wells are again washed, a TMB substrate solution is added to the wells and color develops in proportion to the amount of VEGFR-2 bound. The Stop Solution is added and the intensity of the color is measured at 450 nm. Percent inhibition was calculated by the comparison of compounds treated to control incubations. The concentration of the test compound causing 50% inhibition (IC_{50}) was calculated from the concentration inhibition response curve and the data were compared with sorafenib as standard VEGFR-2 inhibitor

4.3. Molecular Docking study

Molecular docking simulation study was carried out using Molecular Operating Environment (MOE, 10.2008) software. All minimizations were performed with MOE until an RMSD gradient of 0.05 kcal·mol^{-1}Å^{-1} with MMFF94x force field and the partial charges were automatically calculated. The X-ray crystallographic structure of VEGFR-2 co-crystallized with sorafenib as inhibitor (PDB ID: 4ASD) was downloaded from the protein data bank http://www.rcsb.org/ [40].Water molecules were removed, then the receptor was prepared for docking study using *Protonate 3D* protocol in MOE with default options. The co-crystalized ligand was used to define the active site for docking. Triangle Matcher placement method and London dG scoring function were used for docking.

Docking protocol was first validated by re-docking of the co-crystallized ligand (Sorafenib) in the vicinity of the active site of the receptor with energy score (S) = −15.19 kcal/mol and RMSD of 0.470Å. The validated docking protocol was then used to study the ligand-receptor interactions in the active site for the newly synthesized compounds to predict their binding mode and binding affinity.

Acknowledgement

This study was supported by the National Research Centre fund through the project No 10010102. Deep thanks are expressed to the 'Science and Technology Development Fund' for financially supporting the manuscript through the project ID 1517. The authors are grateful to the National Cancer Institute, Cancer Biology Department, Cairo, Egypt, for performing the cytotoxic evaluation against MCF-7 and HepG2. Special thanks to the confirmatory diagnostic unit, VACSERA-Egypt for testing the compounds for their VEGFR-2 inhibitory activity. 3D Molecular graphics in the discussion and results section were generated using the UCSF Chimera package. [41] Chimera is developed by the Resource for Biocomputing, Visualization, and Informatics at the University of California, San Francisco, supported by grants from the National Institutes of Health National Center for Research Resources (2P41RR001081) and National Institute of General Medical Sciences (9P41GM103311).

References

[1] J.F. López-Sáez, C. de la Torre, J. Pincheira, G. Giménez-Martín, Cell proliferation and cancer, Histol. Histopathol. 13 (1998) 1197-1214.

[2] J. Folkman, Angiogenesis in cancer, vascular, rheumatoid and other disease, Nat. Med. 1 (1995) 27-31.

[3] R.S. Kerbel, Tumor angiogenesis: past, present and the near future, Carcinogenesis 21 (2000) 505-515.

[4] A.F. Karamysheva, Mechanisms of angiogenesis, Biochemistry (Moscow). 73 (2008) 751-762.

[5] P. Traxler, Tyrosine kinases as targets in cancer therapy - successes and failures, Expert Opin. Ther. Targets 7 (2003) 215-234.

[6] L.K. Shawver, K.E. Lipson, T.A.T. Fong, G. McMahon, G.D. Plowman, L.M. Strawn, Receptor tyrosine kinases as targets for inhibition of angiogenesis, Drug Discov. Today. 2 (1997) 50-63.

[7] K. Holmes, O.L. Roberts, A.M. Thomas, M.J. Cross, Vascular endothelial growth factor receptor-2: structure, function, intracellular signalling and therapeutic inhibition, Cell Signal. 19 (2007) 2003-2012.

[8] N. Ferrara, H.P. Gerber, J. LeCouter, The biology of VEGF and its receptors, J. Nat. Med. 9 (2003) 669-676.

[9] M. Simons, E. Gordon, L. Claesson-Welsh, Mechanisms and regulation of endothelial VEGF receptor signaling, Nat. Rev. Mol. Cell Biol. 10 (2016) 611-625.

[10] K.M. Sakamoto, Su-11248 Sugen Drugs, Curr. Opin. Investig. 5 (2004) 1329-1339.

[11] K. Podar, L.P. Catley, Y.T. Tai, R. Shringarpure, P. Carvalho, T. Hayashi, R. Burger, R.L. Schlossman, P.G. Richardson, L.N. Pandite, R. Kumar, T. Hideshima, D. Chauhan, K.C. Anderson, GW654652, the pan-inhibitor of VEGF receptors, blocks the growth and migration of multiple myeloma cells in the bone marrow microenvironment, Blood 9 (2004) 3474-3479.

[12] T. Ahman, T. Eisen, Kinase inhibition with BAY 43-9006 in renal cell carcinoma, Clin. Cancer Res. 10 (2004) 6388-6392.

[13] P. Wu, T.E. Nielsen, M.H. Clausen, FDA-approved small-molecule kinase inhibitors, Trends Pharmacol. Sci. 36 (2015) 422–439.

[14] R. Jr. Roskoski, VEGF receptor protein-tyrosine kinases: structure and regulation, Biochem. Biophys. Res. Commun. 375 (2008) 287-291.

[15] F. Zuccotto, E. Ardini, E. Casale, M. Angiolini, Through the “gatekeeper door”: exploiting the active kinase conformation, J. Med. Chem. 53 (2010) 2681-2694.

[16] L. Lintnerová, M. García-Caballero, F. Gregáň, M. Melicherčík, A.R. Quesada, J. Lác, M. Sališová, A. Boháč, A development of chimeric VEGFR2 TK inhibitor based on two ligand conformers from PDB: 1Y6A complex--medicinal chemistry consequences of a TKs analysis, Eur. J. Med. Chem. 24 (2014) 146-159.

[17] Z. Zhao, H. Wu, L. Wang, Y. Liu, S. Knapp, Q. Liu, N.S. Gray, Exploration of Type II Binding Mode: A Privileged Approach for Kinase Inhibitor Focused Drug Discovery?, ACS Chemical Biology 9 (2014) 1230-1241.

[18] H.-Q Zhang, F.-H Gong, C.-G Li, C. Zhang, L.-P. Sun, Design and discovery of 4-anilinoquinazoline-acylamino derivatives as EGFR and VEGFR-2 dual TK inhibitors, Eur. J. Med. Chem. 109 (2016) 371-379.

[19] J.R. Simard, D. Rauh, Screening for allosteric kinase inhibitors in high-throughput: A novel fluorescence approach for detecting DFG-out kinase inhibitors. Screening-Trends in Drug Discovery l3 (2009) 2-4.

[20] W. Eldehna, S. Abou-Seri, A.M. El Kerdawy, R.R. Ayyad, A.M. Hamdy, H.A. Ghabbour, M.M. Ali, D.A. Abou El Ella, Increasing the binding affinity of VEGFR-2 inhibitors by extending their hydrophobic interaction with the active site: Design, synthesis and biological evaluation of 1-substituted-4-(4-methoxybenzyl)phthalazine derivatives, Eur. J. Med. Chem. 113 (2016) 50-62.

[21] M.K. Amin, F.F. Barsoum, M.F. Awadallah, E.N. Mohamed, phthalazine derivatives with VEGFR-2 and EGFR kinase inhibitory activity, Eur. J. Med. Chem. 123 (2016) 191-201

[22] T. Zhichao, W. Chengzhe, W. Tianlin, L. Kejing, X. Hua, Design, synthesis and evaluation of 6-aryl-indenoisoquinolone derivatives dual targeting ER<alpha> and VEGFR-2 as anti-breast cancer agents, Eur. J. Med. Chem. 118 (2016) 328-339

[23] Z. Jin, J. Xiangdong, J. Yingnan, G. Mingrui, Recent advances in the development of dual VEGFR and c-Met small molecule inhibitors as anticancer drugs, Eur. J. Med. Chem.108 (2016) 495-504

[24] K. Lin, j. Lien, C. Chung, S. Kuo, T. Huang, A Novel Compound, NP-184, Inhibits the Vascular Endothelial Growth Factor Induced Angiogenesis, Eur. J. Pharmacol. 630 (2010) 53-60.

[25] H.L. Kuo, J.C. Lien, C.H. Chung, C.H. Chang, S.C. Lo, I.C. Tsai, H.C. Peng, S.C. Kuo, T.F. Huang, NP-184 [2-(5-methyl-2-furyl) benzimidazole], A novel orally active antithrombotic agent with dual antiplatelet and anticoagulant activities, Naunyn. Schmiedebergs. Arch. Pharmacol. 381 (2010) 495-505.

[26] S.W. Huang, J.C. Lien, S.C. Kuo, T.F. Huang, Antiangiogenic mechanisms of PJ-8, a novel inhibitor of vascular endothelial growth factor receptor signaling, Carcinogenesis. 33 (2012) 1022-1030.

[27] A. Temirak, Y.M. Shaker, F.A. Ragab, M.M. Ali, S.M. Soliman, J. Mortier, G. Wolber, H.I. Ali, H.I. El Diwani, Synthesis, Biological Evaluation, and Docking Studies of New 2-Furylbenzimidazoles as Anti-Angiogenic Agents: Part II, Arch. Pharm. Chem. Life Sci. 347 (2014) 291-304.

[28] A. Temirak, Y.M. Shaker, F.A. Ragab, M.M. Ali, H.I. Ali, H.I. El Diwani, Part I. Synthesis, biological evaluation and docking studies of new 2-furylbenzimidazoles as antiangiogenic agents, Eur. J. Med. Chem. 87 (2014) 868 – 880.

[29] V.J. Cee, A.C. Cheng, K. Romero, S. Bellon, C. Mohr, D.A. Whittington, A. Bak, J. Bready S. Caenepeel, A. Coxon, H.L. Deak, J. Fretland, Y. Gu, B.L. Hodous, X. Huang, J.L. Kim, J. Lin, A.M. Long, H. Nguyen, P.R. Olivieri, V.F. Patel, L. Wang, Y. Zhou, P. Hughes, S. Geuns-Meyer, Pyridyl-pyrimidine benzimidazole derivatives as potent, selective, and orally bioavailable inhibitors of Tie-2 kinase, Bioorg. Med. Chem. Lett. 19 (2009) 424–427.

[30] H.F. Ridley, R.G.W. Spickett, G.M. Timmis, New synthesis of benzimidazoles and aza-analogs, J. Heterocycl. Chem. 2 (1965) 253-256.

[31] B. G. Alunni, G. De Meo, M. Pedini, A. Ricci, M. Pitzurra, R. Cavallo, T. Sposini, P. Jacquignon, New heterocyclic derivatives of benzimidazole with germicidal activity, Farmaco Sci. 37 (1982) 597-611.

[32] P. Skehan, R. Storeng, D. Scudiero, A. Monks, J. McMahon, D. Vistica, J.T. Warren, H. Bokesch, S. Kenney, M.R. Boyd, New colorimetric cytotoxicity assay for anticancer-drug screening., J. Natl. Cancer Inst. 82 (1990) 1107-1112.

[33] A. Monks, D. Scudiero, P. Skehan, R. Shoemaker, K. Paull, D. Vistica, C. Hose, J. Langley, P. Cronise, A. Vaigro-Wolff, Feasibility of a high-flux anticancer drug screen using a diverse panel of cultured human tumor cell lines, J. Natl. Cancer Inst. 83 (1991) 757-766.

[34] H.M. Verheul, E.E. Voest, R.O. Schlingemann, Are tumours angiogenesis-dependent?, J. Pathol. 202 (2004) 5-13.

[35] K.J. Gotink, H.M. Verheul, Anti-angiogenic tyrosine kinase inhibitors: what is their mechanism of action?, Angiogenesis. 13 (2010) 1-14.

[36] G. Shanchun, S.C. Laronna, F. Miles, Z. Yuanyuan, R.G. Ruben, Vascular Endothelial Growth Factor Receptor -2 in Breast Cancer, Biochim. Biophys. Acta 1806 (2010) 108–121.

[37] T. Mele, D. Generali, S. Fox, M.P. Brizzi, A. Bersiga, M. Milani, G. Allevi, S. Bonardi, S. Aguggini, M. Volante, L. Dogliotti, A. Bottini, A. Harris, A. Berruti, Anti-angiogenic effect of tamoxifen combined with epirubicin in breast cancer patients, Breast Cancer Res. Treat. 123 (2010)795–804.

[38] J.S. Shim, R.J. Li, J. Lv, S.A. Head, E.J. Yang, J.O Liu, Inhibition of angiogenesis by selective estrogen receptor modulators through blockade of cholesterol trafficking rather than estrogen receptor antagonism, Cancer Lett. 362 (2015) 106-115.

[39] M. McTigue, B.W. Murray, J.H. Chen, Y.L. Deng, J. Solowiej, R.S. Kania, Molecular conformations, interactions, and properties associated with drug efficiency and clinical performance among VEGFR TK inhibitors, Proc. Natl. Acad. Sci. U S A. 109 (2012) 18281–18289.

[40] http://www.rcsb.org/

[41] E.F. Pettersen, T.D. Goddard, C.C. Huang, G.S. Couch, D.M. Greenblatt, E.C. Meng, T.E. Ferrin, UCSF chimera - A visualization system for exploratory research and analysis, J. Comput. Chem. 13 (2004) 1605-1612

Highlights

Design, Synthesis, Molecular Docking and Cytotoxic Evaluation of Novel 2-Furybenzimidazoles as VEGFR-2 Inhibitors

Mona A. Abdullaziz,[a] **Heba T. Abdel-Mohsen,***[a] **Ahmed M. El Kerdawy,**[b,c] **Fatma A. F. Ragab,**[b] **Mamdouh M. Ali**,[d] **Sherifa M. Abu-bakr,**[a] **Adel S. Girgis,**[e] **Hoda I. El Diwani**[a]

- In the present study, a novel series of benzimidazol-furan hybrids was designed and synthesized through facile synthetic pathways.
- Most of the synthesized compounds showed interesting cytotoxic activity against two cancer cell lines (MCF-7 & HepG2) in comparison to tamoxifen or cisplatin.
- *In vitro* evaluation of the synthesized compounds for their effect on the level of VEGFR-2 in MCF-7 cell line showed their potent inhibitory activity relative to control untreated cells.
- Molecular docking was performed to study the binding pattern of the newly synthesized compounds with VEGFR-2 active site. Structure-activity relationship (SAR) was inferred for future optimization based on the performed biological and docking studies.